Inversion of Sun & Sky Radiance to Derive Aerosol Properties from AERONET

Oleg Dubovik (GEST/UMBC, NASA/GSFC)

Contributors: Brent Holben, Alexander Smirnov, Tom Eck, Ilya Slutsker, Tatyana Lapyonok, AERONET

University of Maryland, College Park, February 20, 2003

Outlines of presentation:

***1. Introduction*: what is the strength of aerosol retrieval from the ground?**

2. Role and place of the retrieval algorithm in AERONET data flows.

3. Inversion* of radiance into aerosol properties*:

- **Forward modeling of atmospheric radiance**
- **Numerical inversion**
- **Products of radiance inversion**

***4. Results: absorption, size and refractive index* of aerosols:**

- **multi-year retrievals for various aerosols;**
- **observed tendencies in aerosol retrievals**

***5. Achievements & Problems* of *AERONET* aerosol retrievals:**

- **sensitivity to instrumental offsets, etc.;**
- **effects of particle inhomogeneity and non-sphericity**

6. Accounting for aerosol particle shape in AERONET retrieval

***7. Conclusion:* achivements and perspectives**

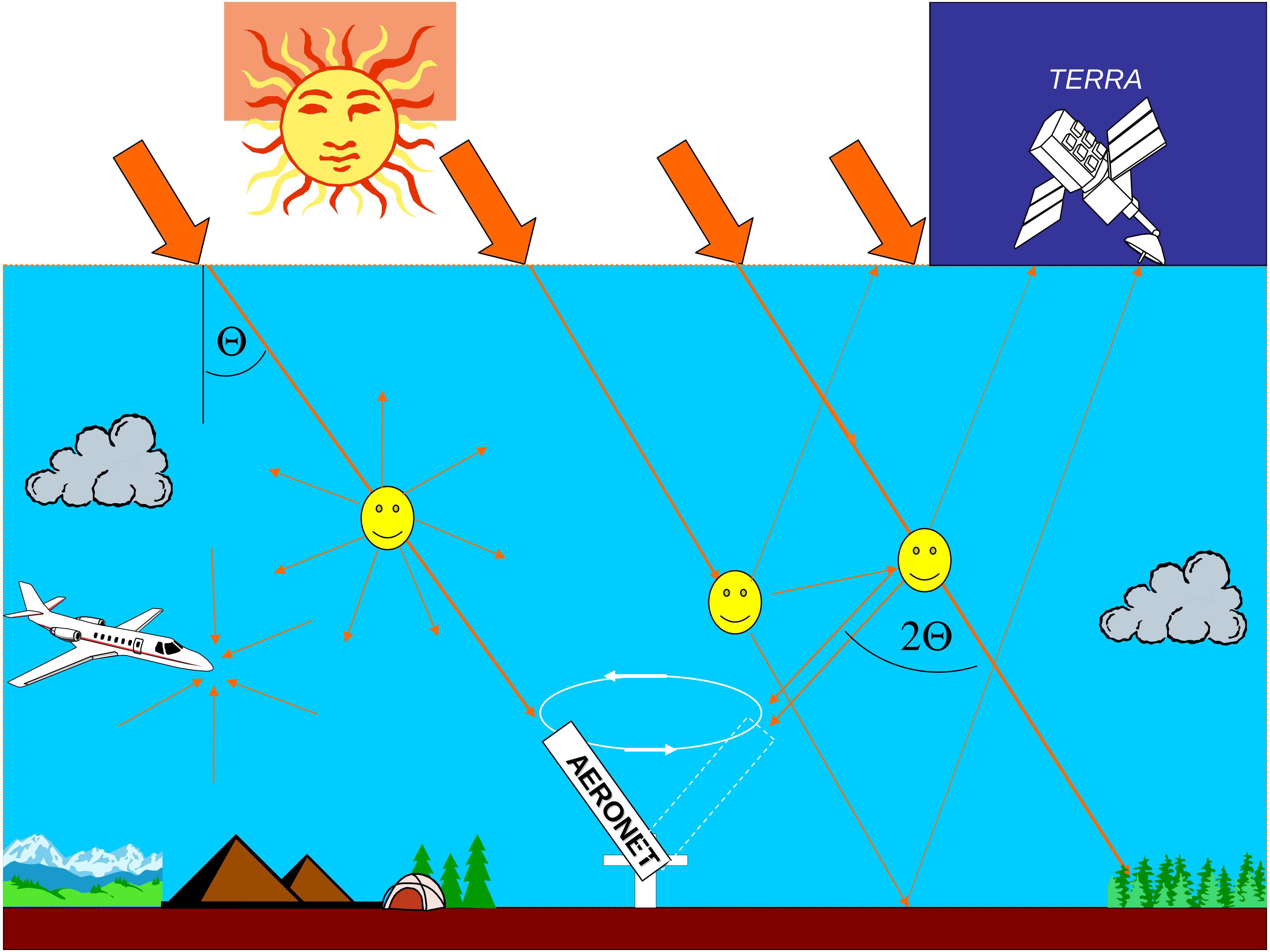

TERRA
Θ
2Θ
AERONET

Surface remote sensing compare to satellite and in-situ measurements

	Advantages	Disadvantages
Ground-based remote sensing:	- high information on aerosol ($0^o \leq \Theta_{scat} \leq 150^o$; transmitted light dominates over reflected); - non-intrusive measurements; - easy access to equipment;	- local coverage; - limited vertical and back-scattering information; - indirect measurements; - very limited capability in presence of clouds
Satellite remote sensing:	- global coverage; - non-intrusive measurements	- limited on information aerosol ($45^o \leq \Theta_{scat}$; aerosol and surface effects to be separated); - no access to equipment
In-situ measurements:	- very straightforward; - unique aerosol physical and chemical information; - universal applicability - (e.g. in cloudy atmosphere);	- intrusive measurements; - local coverage

The main strength of remote sensing from ground for characterization of aerosol and radiation ?

Because, it provides most accurate information regarding aerosol abilities to change atmospheric radiation, i.e. about :

- aerosol loading ($\tau(\lambda)$ - aerosol optical thickness);

- angular distribution of aerosol scattering (P$(\Theta;\lambda)$ - phase function);

-degree of aerosol absorption ($\omega_0(\lambda)$ -single scattering albedo)

***AERONET** (AErosol RObotic NETwork)-*

CENTRE NATIONAL DE LA RECHERCHE SCIENTIFIQUE

An internationally Federated Network

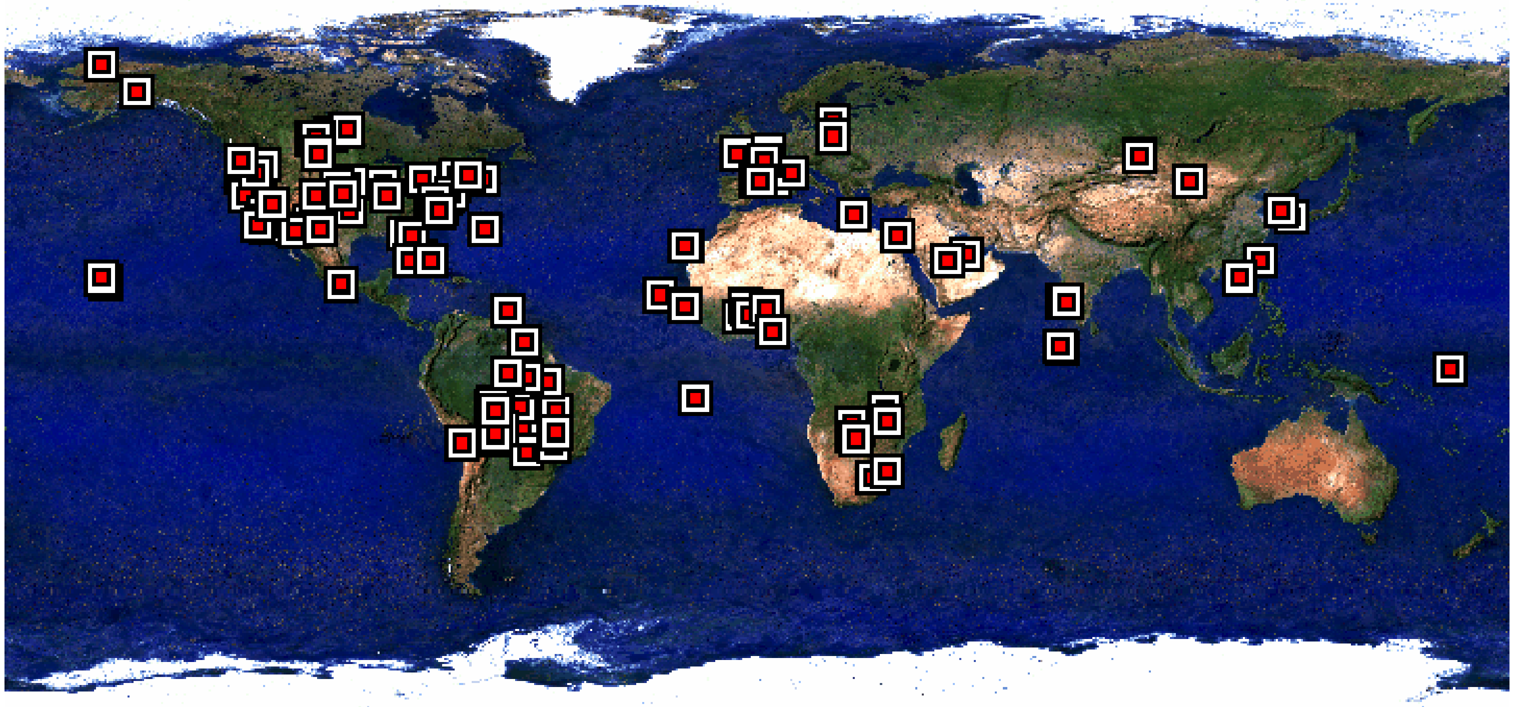

SeaWiFS composite

LDOPE / MODLAND

- *Characterization of aerosol optical properties*
- *Validation of satellite aerosol retrieval*
- *Near real-time acquisition; long term measurements*
- *Homepage access: http://aeronet.gsfc.nasa.gov*

AERONET data flows:

Flux and radiance measurements:

Direct (λ = 340, 380, 440, 500, 670, 870, 1020nm)

Diffuse(λ=440,670,870,1020nm; $2^o \leq \Theta_{sct} \leq 2\Theta_{sun}$)

Holben et al. [1998]

Calibration and maintenance Information

Holben et al. [1998]

Computation of τ_{aer} and $\mathbf{I}(\lambda;\Theta)$:

Holben et al. [1998]

τ_{aer}(λ = 340, 380, 440, 500, 670, 870, 1020nm)

I(λ = 440, 670, 870, 1020nm; $2^o \leq \Theta_{sct} \leq 2\Theta_{sun}$)

Internal quality checks and cloud screening

Holben et al. [1998]

Smirnov et al. [2000]

Retrieval Results:

τ_{aer}(λ = 340, 380, 440, 500,670, 870,1020nm)

Parameters of fine and coarse modes of dV/dlnR

Eck et al. [1999],*O'Neill et al.* [2000]

Inversion of $\tau_{aer}(\lambda)$ and $\mathbf{I}(\lambda;\Theta)$

(λ = 440, 670, 870, 1020; $\Theta_{sct} \leq 2\Theta_{sun}$)

Into particle sizes & refractive index

Dubovik and King [2000]

Nakajima et al.[1996]

dV(r)/dlnR ($0.05 \leq r \leq 15\mu m$)

n(λ), k(λ), ω_o(λ), P(λ,Θ),

<cos(Θ)>, etc (λ=440,670,870,1020)

Dubovik et al.[2000]

Retrieval scheme:

forward model of the observations:

fitting of observations by forward model

observations

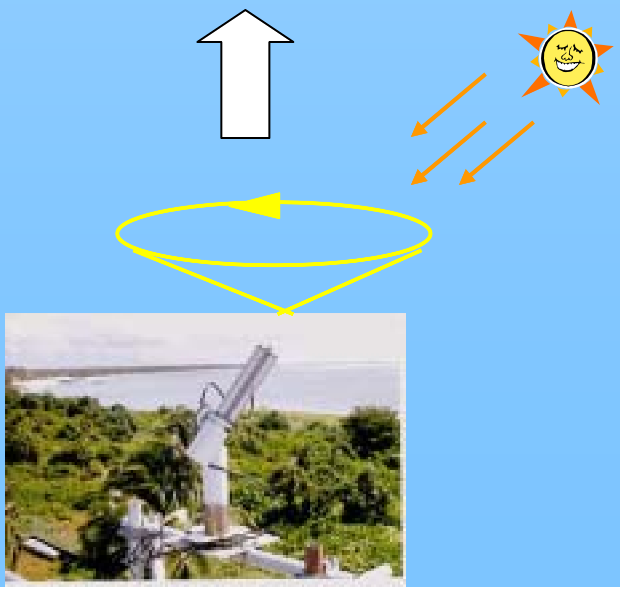

aerosol particle sizes, refractive index, single scattering albedo**, **etc.

Multiple Scattering

Multiple scattering effects are accounted by solving *scalar* radiative transfer equation with assuming *Lambertian ground reflectance* (Nakajima – Tanaka code)

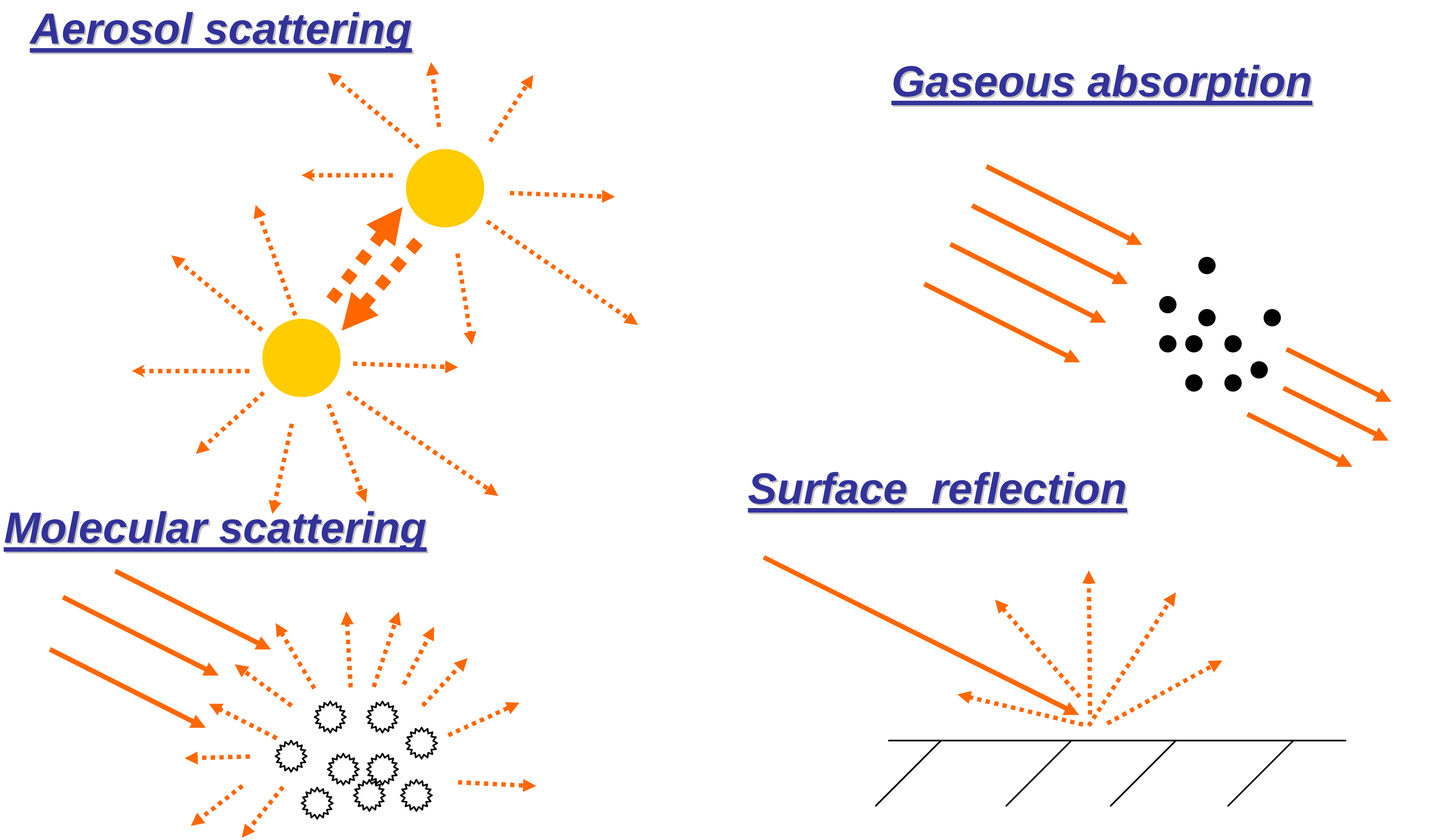

Single Scattering by Single Particle

Scattering and Absorption *is modeled assuming aerosol particle as homogeneous sphere with spectrally dependent complex refractive index ($m(\lambda) = n(\lambda) - i\,k(\lambda)$) - "Mie particles"*

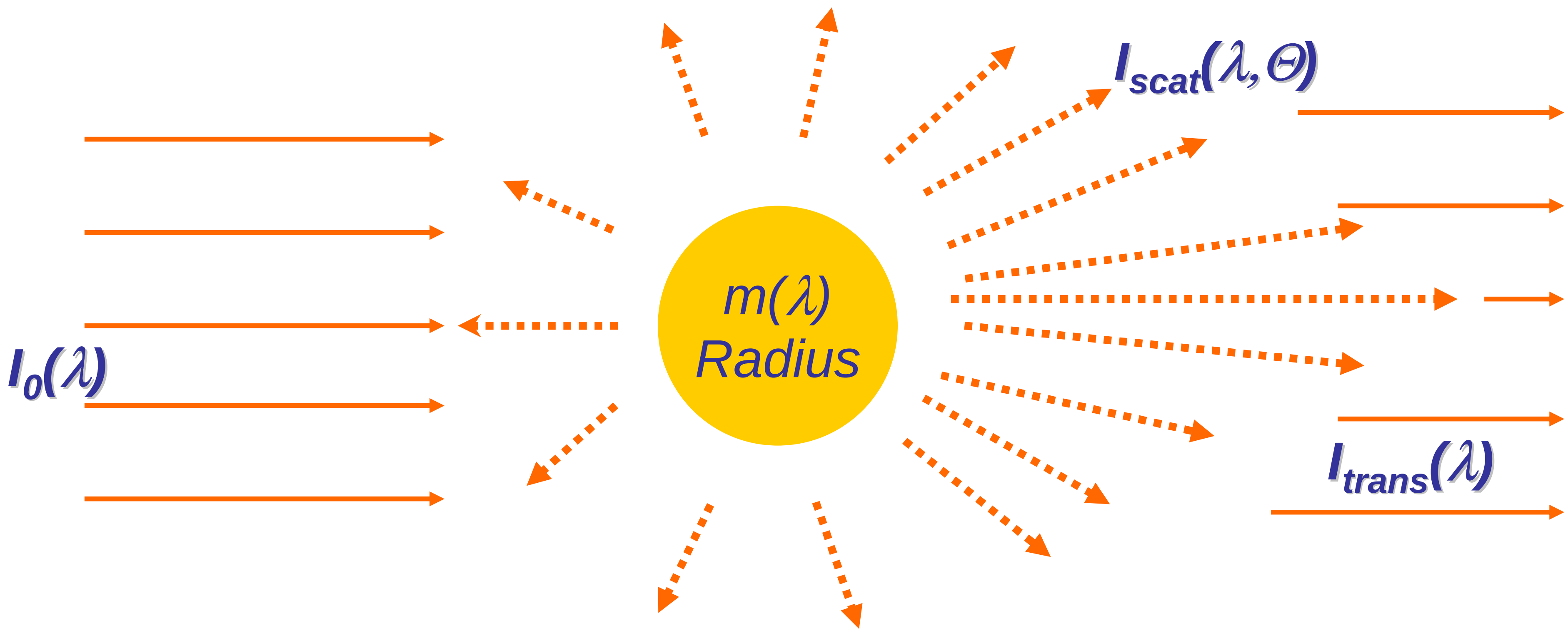

P(Θ)- Phase Function; ***$\omega_0(\lambda)$ -single scattering albedo***

$\tau(\lambda)$ - extinction optical thickness; ***$\tau(\lambda)\omega_0(\lambda)$ absorption optical thickness***

***INPUT* of Forward Model**

Single scattering: aerosol particles - homogeneous spheres

Particle Size Distribution:
0.05 μm ≤ R (22 bins) ≤ 15 μm

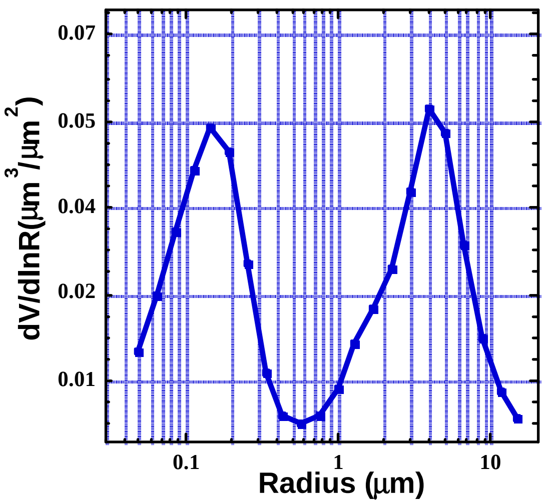

Complex Refractive Index at
λ = 0.44; 0.67; 0.87; 1.02 μm

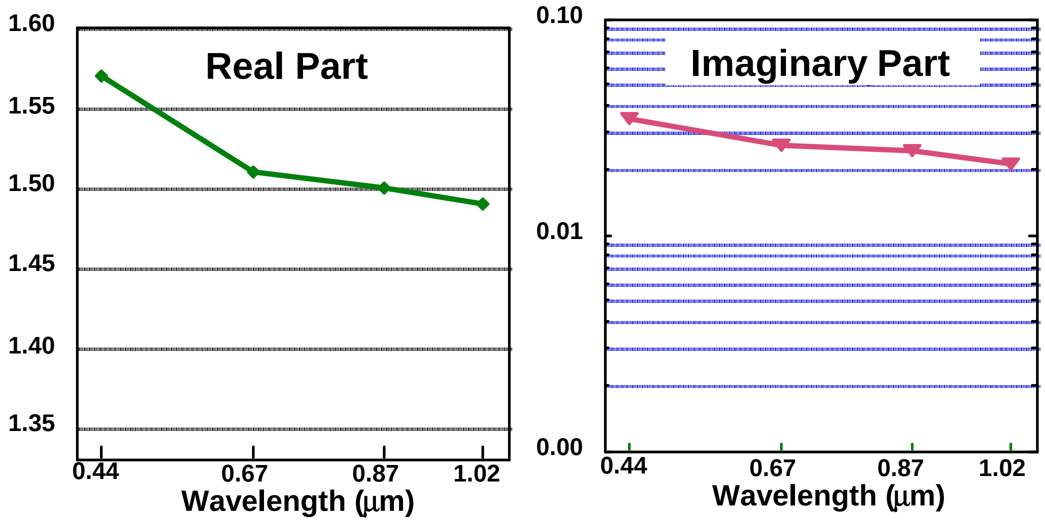

Multiple scattering:

scalar radiative transfer with Lambertian ground reflectance solved by DisOrds (Nakajima-Tanaka or Stamnes et al.)

Inversion Procedure

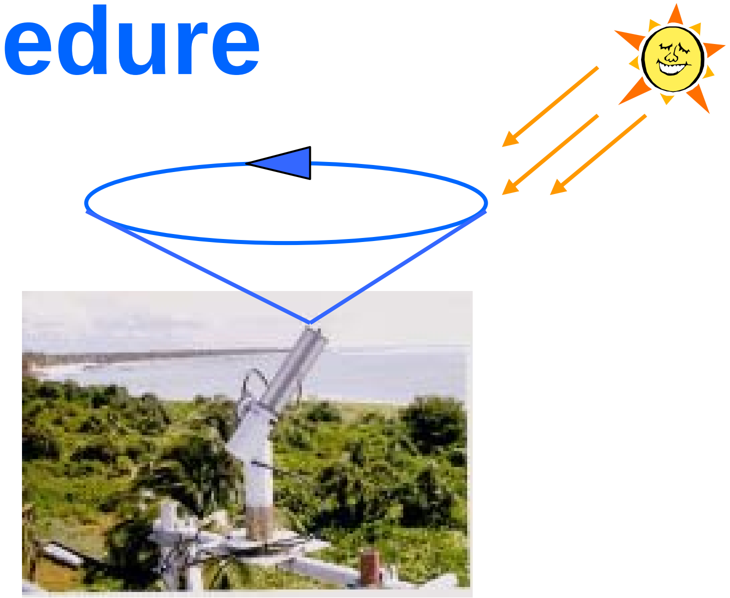

Measurements : **$\tau(\lambda)$ and $I(\lambda,\Theta)$**

$\lambda = 0.44, 0.67, 0.87, 1.02\ \mu m$

$2^o \leq \Theta \leq 150^o$ (up to 30 angles)

Inversion strategy - **statistically optimized fitting**

(Dubovik and King, 2000)

weighting

Lagrange *parameter*

$$\frac{\varepsilon_{sky}^2}{\varepsilon_i^2} \sum_{(\lambda,\theta)_i} \left(f_i^* - f_i(\mathbf{x})\right)^2 + \frac{\varepsilon_{sky}^2}{\varepsilon_a^2} \sum_j \left(f_j^{\,a} - f_j(\mathbf{x})\right)^2 \rightarrow (\mathrm{N}_{\mathrm{total}} - \mathrm{N}_{\mathrm{x}})\hat{\varepsilon}_{sky}^2$$

measurements

a priori

consistency indicator

Products of AERONET inversions

Microphysics (columnar aerosol):

dV(r)/dlnr - volume (number, area, etc.) particle size distribution

(0.05 μm ≤ *r* ≤ 15 μm)

Standard Parameters of dV(r)/dlnr

- **C_v - volume concentration (t, f, c);**
- **r_v - volume median radius (t, f, c);**
- **ε - standard deviation (t, f, c);**
- **r_{eff} - effective radius (t, f, c);**

(t -total aerosol, f- fine and c- coarse modes)

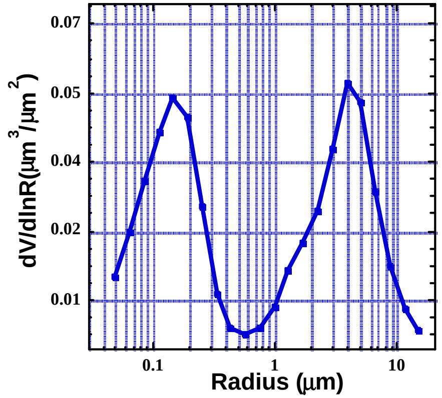

n(λ) - (1.33 ≤ n(λ) ≤ 1.6)

k(λ) - (0.0005 ≤ k(λ) ≤ 0.5)

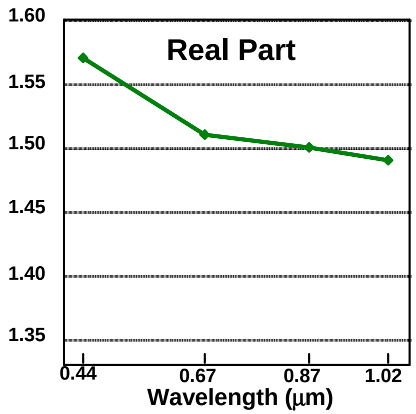

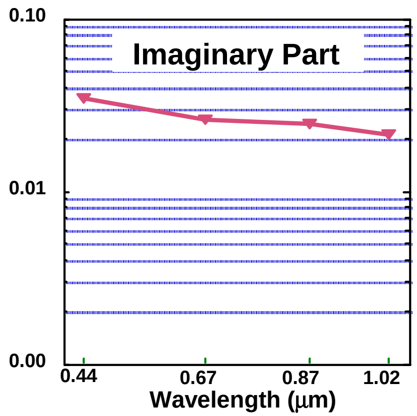

Radiative properties:

- **$\omega_0(\lambda)$ - Single Scattering Albedo**
- **P(Θ; λ) - Phase function (t, f, c);**
- **τ(λ) - Optical thickness (f, c);**
- **F(λ) - Direct and diffuse fluxes ;**

AERONET sky channels:
λ = 0 .44, 0.67, 0.87,1.02 μm

Desert dust

(Bahrain, May 2, 1999)

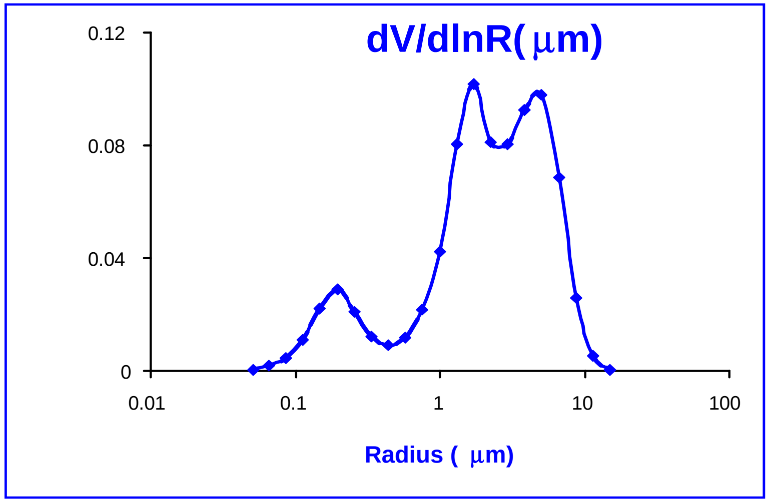

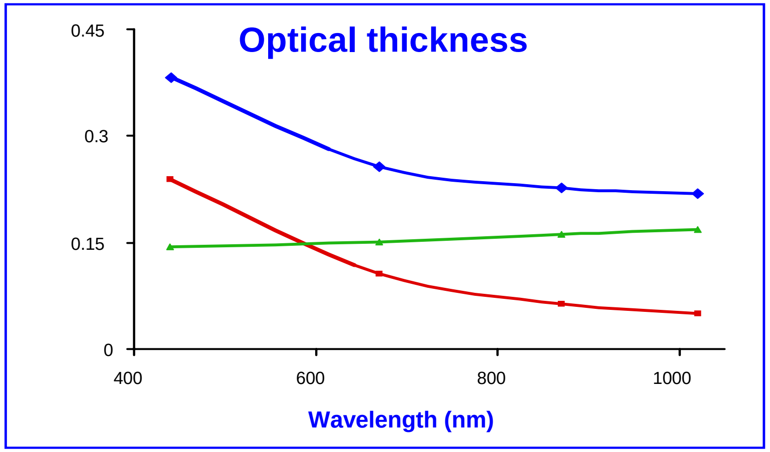

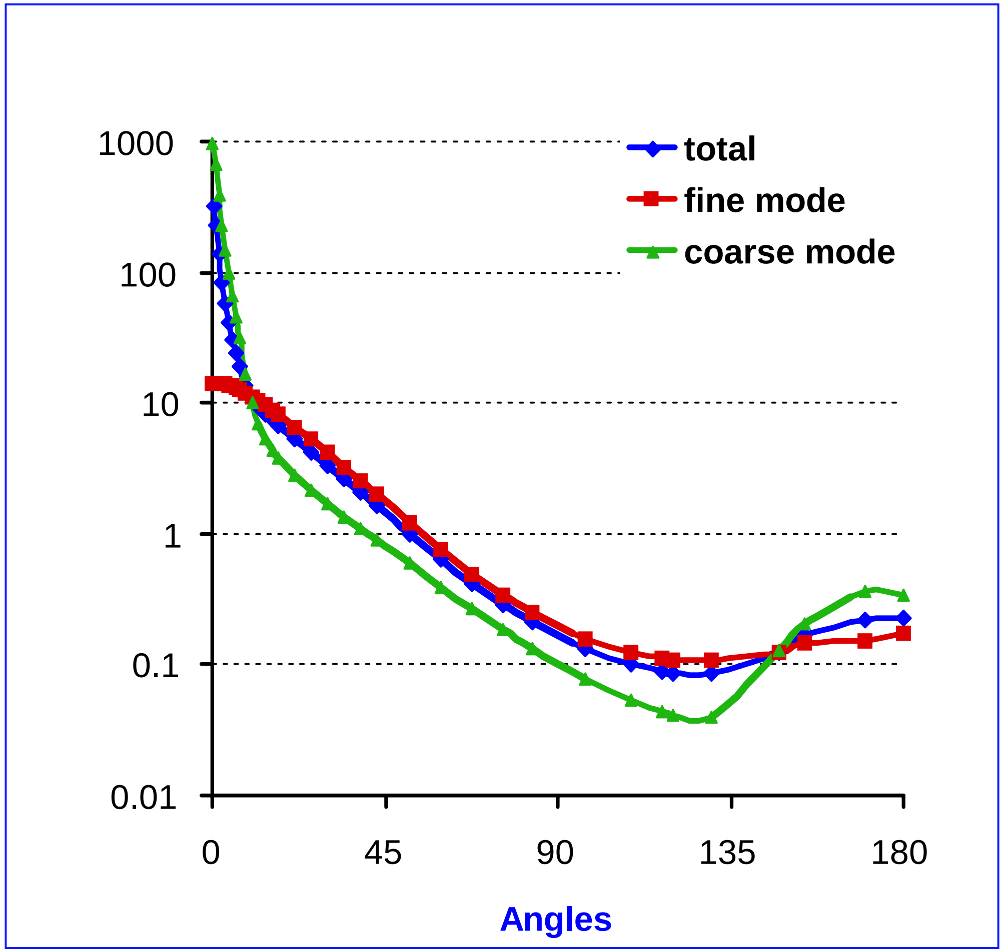

Observation Sites for Climatology

- **- Urban/Industrial** (*GSFC, Paris, Mexico-City, INDOEX*)
- **- Biomass Burning** (*Savanna, Cerrado, Forest*)
- **- Desert Dust** (*Cape Verde, Saudi Arabia, Persian Gulf*)
- **- Oceanic Aerosol** (*Hawaii*)

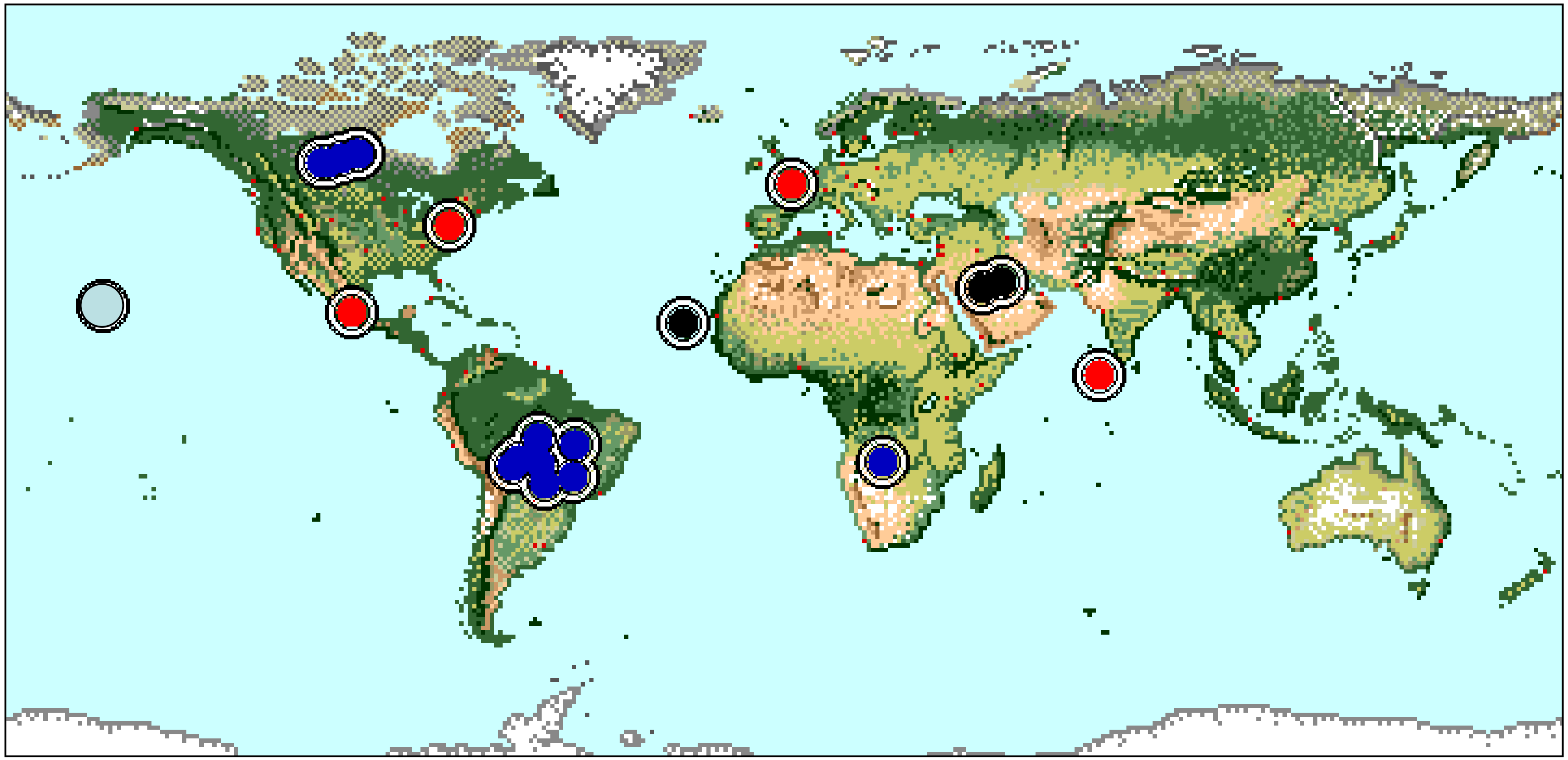

Comparison of Absorption and other Optical Properties for Main Aerosol Types

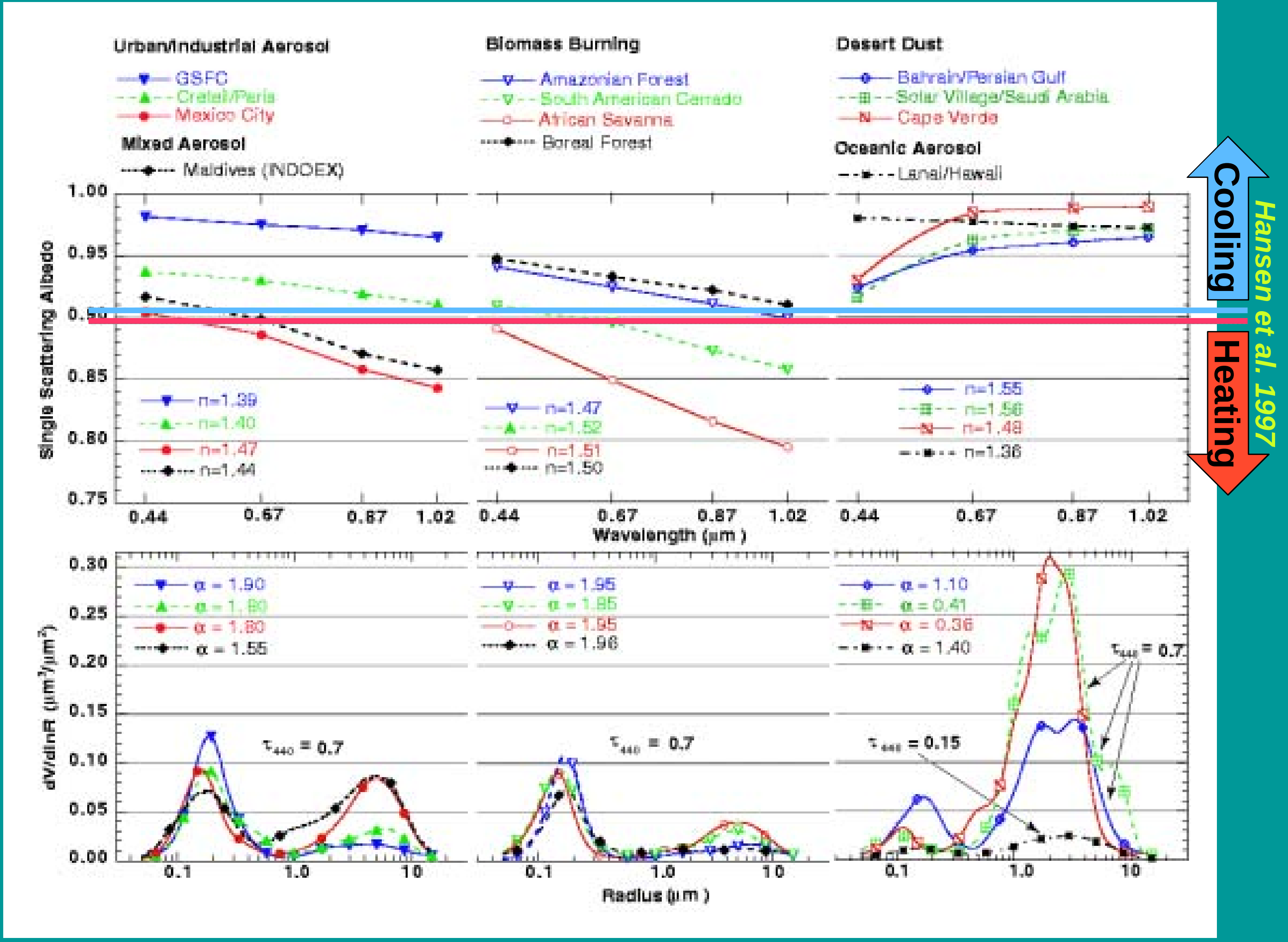

Biospherical Sciences Branch, Science Highlights - May 2002

Table 1. Summary of aerosol optical properties retrieved from worldwide AERONET network of ground-based radiometers.

Urban/Industrial & Mixed:	**GSFC/ Greenbelt /USA** (1993-2000)	**Creteil/ Paris France** (1999)	**Mexico City** (1999 - 2000)	**Maldives (INDOEX)** (1999-2000)
Number of meas. (total)	2400	300	1500	700
Number of meas. (for ω_0, *n*, *k*)	200 (June Š September)	40 (June Š September)	300	150 (January Š April)
Range of optical thickness;$<\tau>$	$0.1 \le \tau(440) \le 1.0$; $<\tau(440)>= 0.24$	$0.1 \le \tau(440) \le 0.9$; $<\tau(440)>= 0.26$	$0.1 \le \tau(440) \le 1.8$; $<\tau(440)>= 0.43$	$0.1 \le \tau(440) \le 0.7$; $<\tau(440)>= 0.27$
Range of €ngstrom parameter	$1.2 \le \alpha \le 2.5$	$1.2 \le \alpha \le 2.3$	$1.0 \le \alpha \le 2.3$	$0.4 \le \alpha \le 2.0$
$<g>$ (440/ 670/ 870/ 1020)	0.68/ 0.59/ 0.54/ 0.53 $\pm$ 0.08			
n; *k*	$1.41 - 0.03\tau(440) \pm 0.01$; 0.003 ± 0.003	1.40 ± 0.03; 0.009 ± 0.004	1.47 ± 0.03; 0.014 ± 0.006	1.44 ± 0.02; 0.011 ± 0.007
ω_0(440/ 670/ 870/ 1020)	0.98/ 0.97/ 0.96/ 0.95 $\pm$0.02	0.94/ 0.93 / 0.92 / 0.91 $\pm$ 0.03	0.90 / 0.88 / 0.85/ 0.83 $\pm$ 0.02	0.91/ 0.89 / 0.86 / 0.84 $\pm$ 0.03
r_{vf} (μm); σ_f	$0.12+0.11\,\tau(440) \pm 0.03$; 0.38 ± 0.01	$0.11+ 0.13\,\tau(440) \pm 0.03$; 0.43 ± 0.05	$0.12 + 0.04\,\tau(440) \pm 0.02$; 0.43 ± 0.03	0.18 ± 0.03; 0.46 ± 0.04
r_{vc} (μm); σ_c	$3.03+0.49\,\tau(440) \pm 0.21$; 0.75 ± 0.03	$2.76 + 0.48\,\tau(440) \pm 0.30$; 0.79 ± 0.05	$2.72 + 0.60\,\tau(440) \pm 0.23$; 0.63 ± 0.05	$2.62 + 0.61\tau(440) \pm 0.31$; 0.76 ± 0.05
C_{vf} ($\mu m^3/\mu m^2$)	$0.15\,\tau(440) \pm 0.03$	$0.01 + 0.12\,\tau(440) \pm 0.04$	$0.12\,\tau(440) \pm 0.03$	$0.12\,\tau(440) \pm 0.03$
C_{vc} ($\mu m^3/\mu m^2$)	$0.01 + 0.04\,\tau(440) \pm 0.01$	$0.01 + 0.05\,\tau(440) \pm 0.02$	$0.11\,\tau(440) \pm 0.03$	$0.15\,\tau(440) \pm 0.04$

Biomass burning:	**Amazonian Forest: Brazil** (1 993-1994); **Bolivia** (1998-1999)**;**	**South American Cerrado: Brazil** (1993-1995)	**African Savanna: Zambia** (1995 - 2000)	**Boreal Forest: USA, Canada** (1994 - 1998)
Number of meas. (total)	700	550	2000	1000
Number of meas. (for ω_0, *n*, *k*)	250 (August Š October)	350 (August Š October)	700 (August Š November)	250 (June Š September)
Range of optical thickness;$<\tau>$	$0.1 \le \tau(440) \le 3.0$; $<\tau(440)>= 0.74$	$0.1 \le \tau(440) \le 2.1$; $<\tau(440)>= 0.80$	$0.1 \le \tau(440) \le 1.5$; $<\tau(440)>= 0.38$	$0.1 \le \tau(440) \le 2.0$; $<\tau(440)>= 0.40$
Range of €ngstrom parameter	$1.2 \le \alpha \le 2.1$	$1.2 \le \alpha \le 2.1$	$1.4 \le \alpha \le 2.2$	$1.0 \le \alpha \le 2.3$
$<g>$ (440/ 670/ 870/ 1020)	0.69/ 0.58/ 0.51/ 0.48 $\pm$ 0.06	0.67/ 0.59/ 0.55/ 0.53 $\pm$ 0.03	0.64/ 0.53/ 0.48/ 0.47 $\pm$ 0.06	0.69/ 0.61/ 0.55/ 0.53 $\pm$ 0.06
n; *k*	1.47 ± 0.03; 0.0093 ± 0.003	1.52 ± 0.01; 0.015 ± 0.004	1.51 ± 0.01; 0.021 ± 0.004	1.50 ± 0.04; 0.0094 ± 0.003
ω_0(440/ 670/ 870/ 1020)	0.94/ 0.93 /0.91/0.90 $\pm$0.02	0.91/ 0.89/ 0.87/ 0.85 $\pm$0.03	0.88 / 0.84 / 0.80 / 0.78 $\pm$0.015	0.94 / 0.935 / 0.92 / 0.91 $\pm$ 0.02
r_{vf} (μm); σ_f	$0.14+0.013\tau(440) \pm 0.01$; 0.40 ± 0.04	$0.14+0.01\tau(440) \pm 0.01$; 0.47 ± 0.03	$0.12 + 0.025\tau(440) \pm 0.01$; 0.40 ± 0.01	$0.15 + 0.015\tau(440) \pm 0.01$; 0.43 ± 0.01
r_{vc} (μm); σ_c	$3.27+0.58\tau\,(440) \pm 0.45$; 0.79 ± 0.06	$3.27+0.51\tau(440) \pm 0.39$; 0.79 ± 0.04	$3.22 + 0.71\tau(440) \pm 0.43$; 0.73 ± 0.03	$3.21+ 0.2\tau(440) \pm 0.23$; 0.81 ± 0.2
C_{vf} ($\mu m^3/\mu m^2$)	$0.12\,\tau(440) \pm 0.05$	$0.1\,\tau(440) \pm 0.06$	$0.12\,\tau(440) \pm 0.04$	$0.01 + 0.1\,\tau(440) \pm 0.04$
C_{vc} ($\mu m^3/\mu m^2$)	$0.05\,\tau(440) \pm 0.02$	$0.04 + 0.03\,\tau(440) \pm 0.03$	$0.09\,\tau(440) \pm 0.02$	$0.01 + 0.03\,\tau(440) \pm 0.03$

Desert Dust & Oceanic:	**Bahrain/ Persian Gulf** (1998 Š2000)	**Solar-Vil./ Saudi Arabia**(1998-2000)	**Cape Verde** (1993 Š2000)	**Lanai/Hawaii** (1995-2000)
Number of meas. (total)	1800	1500	1500	800
Number of meas. (for ω_0, *n*, *k*)	100	250	300	150
Range of optical thickness;$<\tau>$	$0.1 \le \tau(1020) \le 1.2$, $<\tau(1020)>= 0.22$	$0.1 \le \tau(1020) \le 1.5$; $<\tau(1020)>= 0.17$	$0.1 \le \tau(1020) \le 2.0$; $<\tau(1020)>= 0.39$	$0.01 \le \tau(1020) \le 0.2$; $<\tau(1020)>= 0.04$
Range of €ngstrom parameter	$0 \le \alpha \le 1.6$	$0.1 \le \alpha \le 0.9$	$-0.1 \le \alpha \le 0.7$	$0 \le \alpha \le 1.55$
$<g>$ (440/ 670/ 870/ 1020)	0.68/ 0.66/ 0.66/ 0.66 $\pm$ 0.04	0.69/ 0.66/ 0.65/ 0.65 $\pm$ 0.04	0.73/ 0.71/ 0.71/ 0.71 $\pm$ 0.04	0.75/ 0.71/ 0.69/ 0.68 $\pm$ 0.04
n	1.55 ± 0.03	1.56 ± 0.03	1.48 ± 0.05	1.36 ± 0.01
k(440/ 670/ 870/ 1020)	0.0025/ 0.0014 / 0.001/ 0.001 $\pm$ 0.001	0.0029 /0.0013 /0.001/ 0.001 $\pm$ 0.001	0.0025/ 0.0007/ 0.0006/ 0.0006 $\pm$0.001	0.0015 ± 0.001
ω_0(440/ 670/ 870/ 1020)	0.92 / 0.95/ 0.96 / 0.97 $\pm$ 0.03	0.92/ 0.96/ 0.97/ 0.97 $\pm$ 0.02	0.93/ 0.98 /0.99 /0.99 $\pm$ 0.01	0.98/ 0.97 /0.97 /0.97 $\pm$ 0.03
r_{vf} (μm); σ_f	0.15 ± 0.04; 0.42 ± 0.04	0.12 ± 0.05; 0.40 ± 0.05	0.12 ± 0.03; $0.49 + 0.10\,\tau \pm 0.04$	0.16 ± 0.02; 0.48 ± 0.04
r_{vc} (μm); σ_c	2.54 ± 0.04; 0.61 ± 0.02	2.32 ± 0.03; 0.60 ± 0.03	1.90 ± 0.03; $0.63 - 0.10\,\tau \pm 0.03$	2.70 ± 0.04; 0.68 ± 0.04
C_{vf} ($\mu m^3/\mu m^2$)	$0.02 + 0.1\,\tau(1020) \pm 0.05$	$0.02 + 0.02\,\tau(1020) \pm 0.03$	$0.02 + 0.02\,\tau(1020) \pm 0.03$	$0.40\,\tau(1020) \pm 0.01$
C_{vc} ($\mu m^3/\mu m^2$)	$-0.02 + 0.92\,\tau(1020) \pm 0.04$	$-0.02 + 0.98\,\tau(1020) \pm 0.04$	$0.9\,\tau(1020) \pm 0.09$	$0.80\,\tau(1020) \pm 0.02$

Dubovik et al. 2002

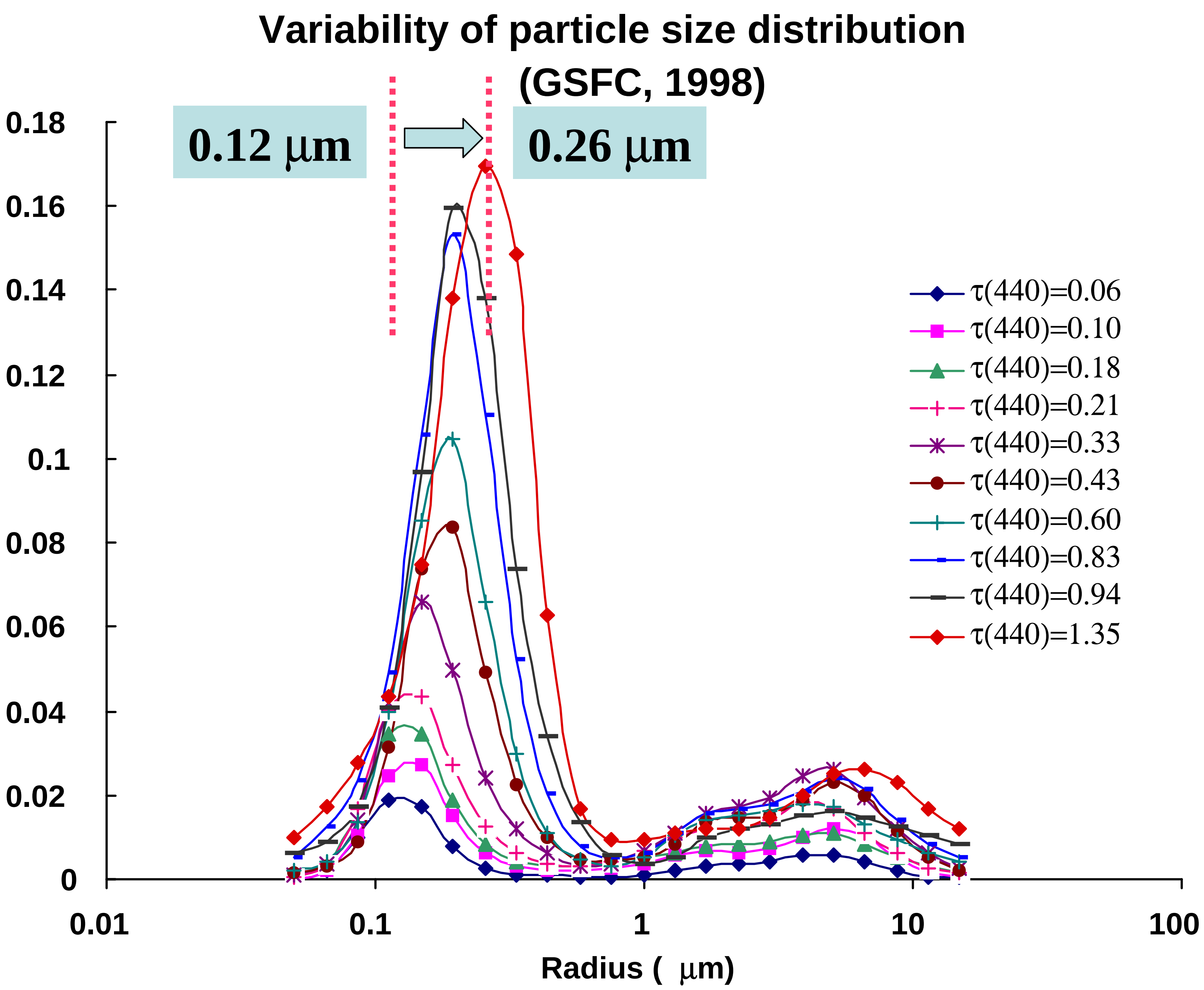

Variability of particle size distribution
(GSFC, 1998)
0.12 μm
0.26 μm
0.18
0.16
0.14
0.12
0.1
0.08
0.06
0.04
0.02
0
0.01
0.1
1
10
100
Radius (μm)
τ(440)=0.06
τ(440)=0.10
τ(440)=0.18
τ(440)=0.21
τ(440)=0.33
τ(440)=0.43
τ(440)=0.60
τ(440)=0.83
τ(440)=0.94
τ(440)=1.35

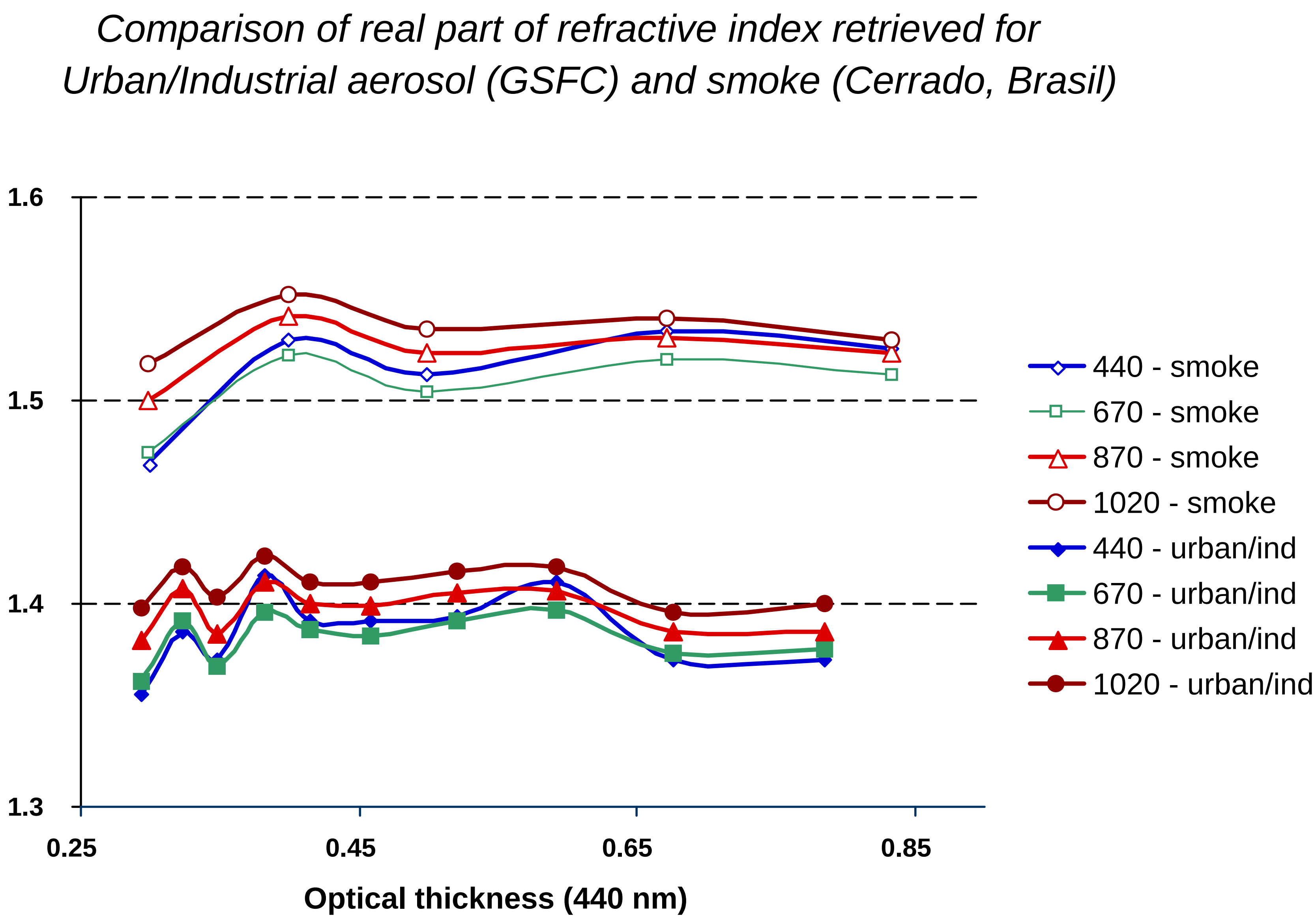
Comparison of real part of refractive index retrieved for
Urban/Industrial aerosol (GSFC) and smoke (Cerrado, Brasil)
1.6
1.5
1.4
1.3
0.25
0.45
0.65
0.85
Optical thickness (440 nm)
440 - smoke
670 - smoke
870 - smoke
1020 - smoke
440 - urban/ind
670 - urban/ind
870 - urban/ind
1020 - urban/ind

Sensitivity to instrumental offsets

Offsets were considered in:

- **optical thickness:** $\Delta\tau(\lambda) = \pm 0.01;\ \pm 0.02;$
- **sky-channel calibration:** $\Delta_I(\lambda;\Theta)/I(\lambda;\Theta)\ 100\% = \pm 5\%;$
- **azimuth angle pointing:** $\Delta\phi = 0.5^o;\ 1^o;$
- **assumed ground reflectance:** $\Delta A(\lambda)/A(\lambda)\ 100\% = \pm 30\%;\ \pm 50\%;$

Aerosol models considered **(bi - modal log-normal):**

- **Water-soluble aerosol for $0.05 \le \tau(440) \le 1$;**
- **Desert dust for $0.5 \le \tau(440) \le 1$;**
- **Biomass burning for $0.5 \le \tau(440) \le 1$;**

Results summary:

- **$\tau(440) \le 0.2$ - $dV/d\ln r$ (+), $n(\lambda)$ (-), $k(\lambda)$ (-), $\omega_0(\lambda)$ (-)**
- **$\tau(440) > 0.2$ - $dV/d\ln r$ (+), $n(\lambda)$ (+), $k(\lambda)$ (+), $\omega_0(\lambda)$ (+)**
- **Angular pointing accuracy is critical for $dV/d\ln r$ of dust**

(+) CAN BE retrieved (-) CAN NOT BE retrieved

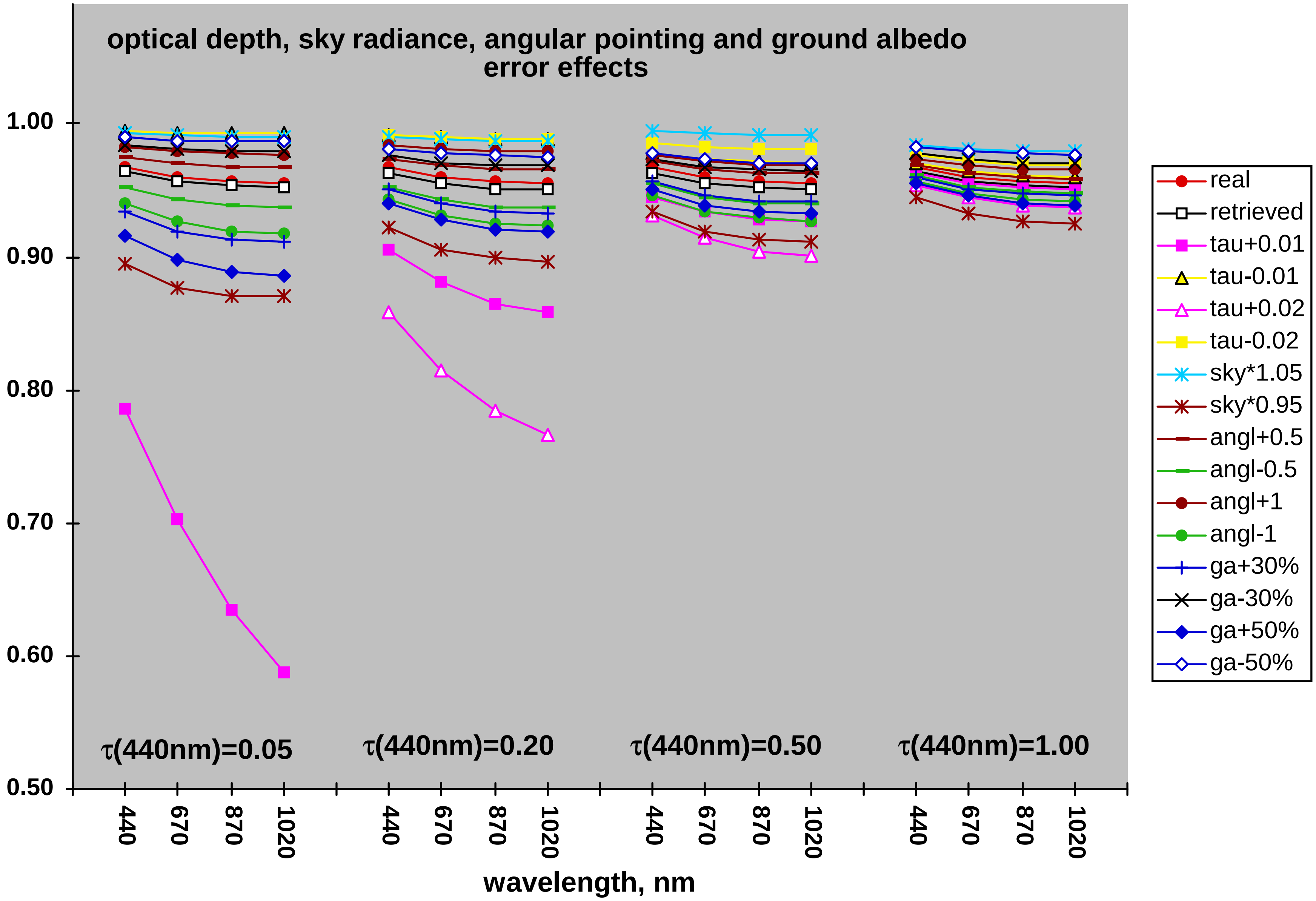

optical depth, sky radiance, angular pointing and ground albedo error effects
1.00
0.90
0.80
0.70
0.60
0.50
τ(440nm)=0.05
τ(440nm)=0.20
τ(440nm)=0.50
τ(440nm)=1.00
440
670
870
1020
wavelength, nm
real
retrieved
tau+0.01
tau-0.01
tau+0.02
tau-0.02
sky*1.05
sky*0.95
angl+0.5
angl-0.5
angl+1
angl-1
ga+30%
ga-30%
ga+50%
ga-50%

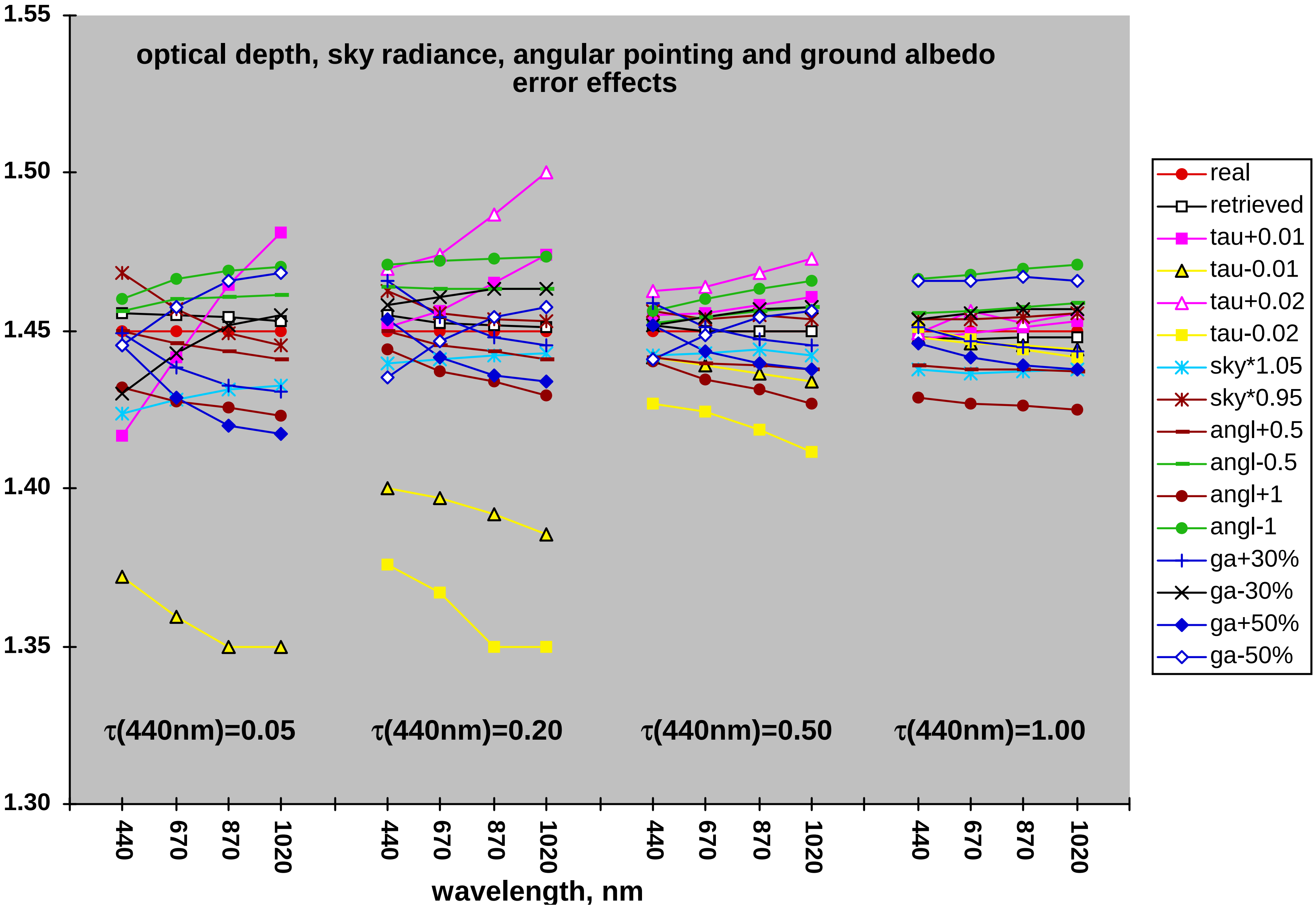

optical depth, sky radiance, angular pointing and ground albedo error effects
1.55
1.50
1.45
1.40
1.35
1.30
τ(440nm)=0.05
τ(440nm)=0.20
τ(440nm)=0.50
τ(440nm)=1.00
440
670
870
1020
wavelength, nm
real
retrieved
tau+0.01
tau-0.01
tau+0.02
tau-0.02
sky*1.05
sky*0.95
angl+0.5
angl-0.5
angl+1
angl-1
ga+30%
ga-30%
ga+50%
ga-50%

Optical model of aerosol

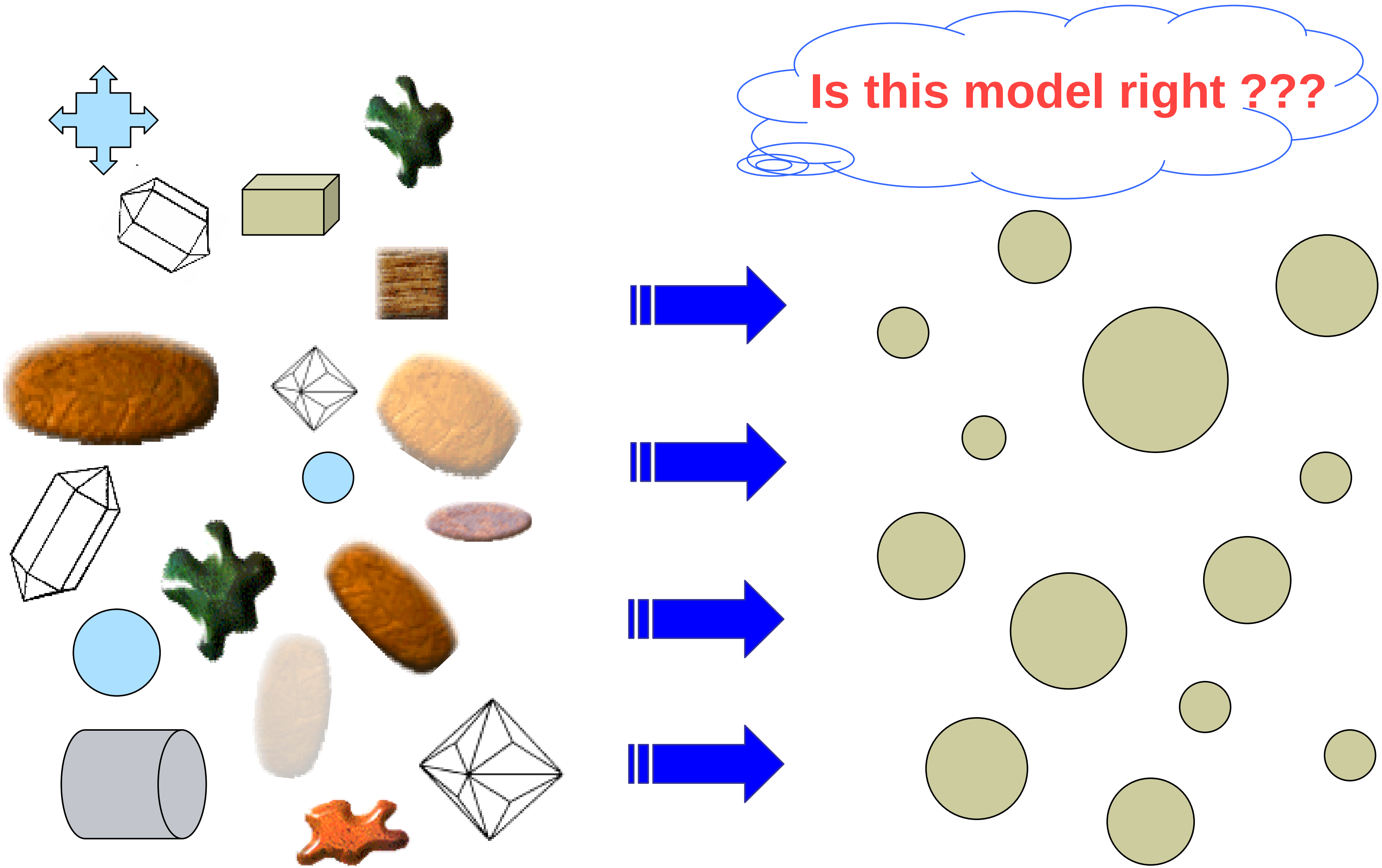

Questioned simplifications:

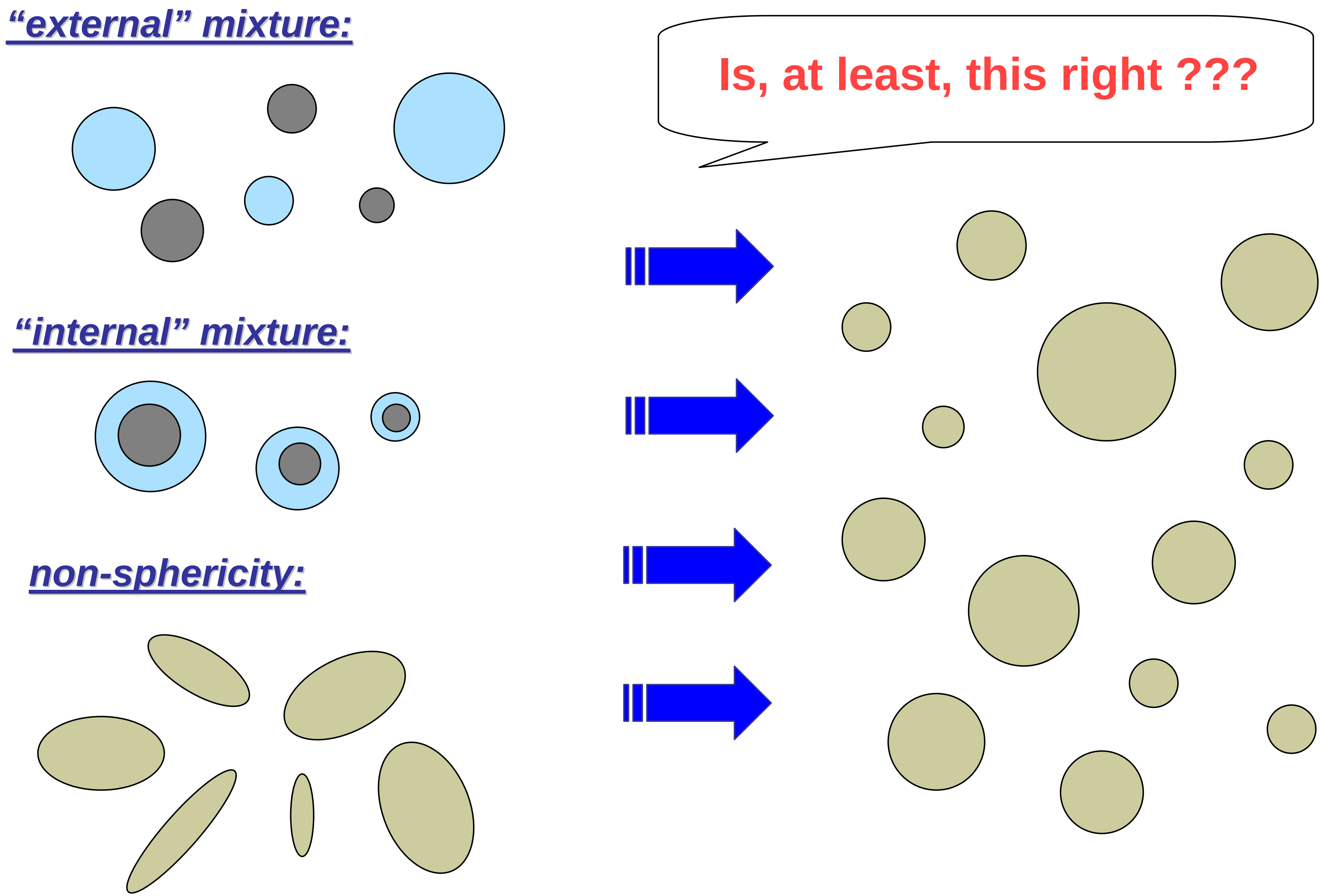

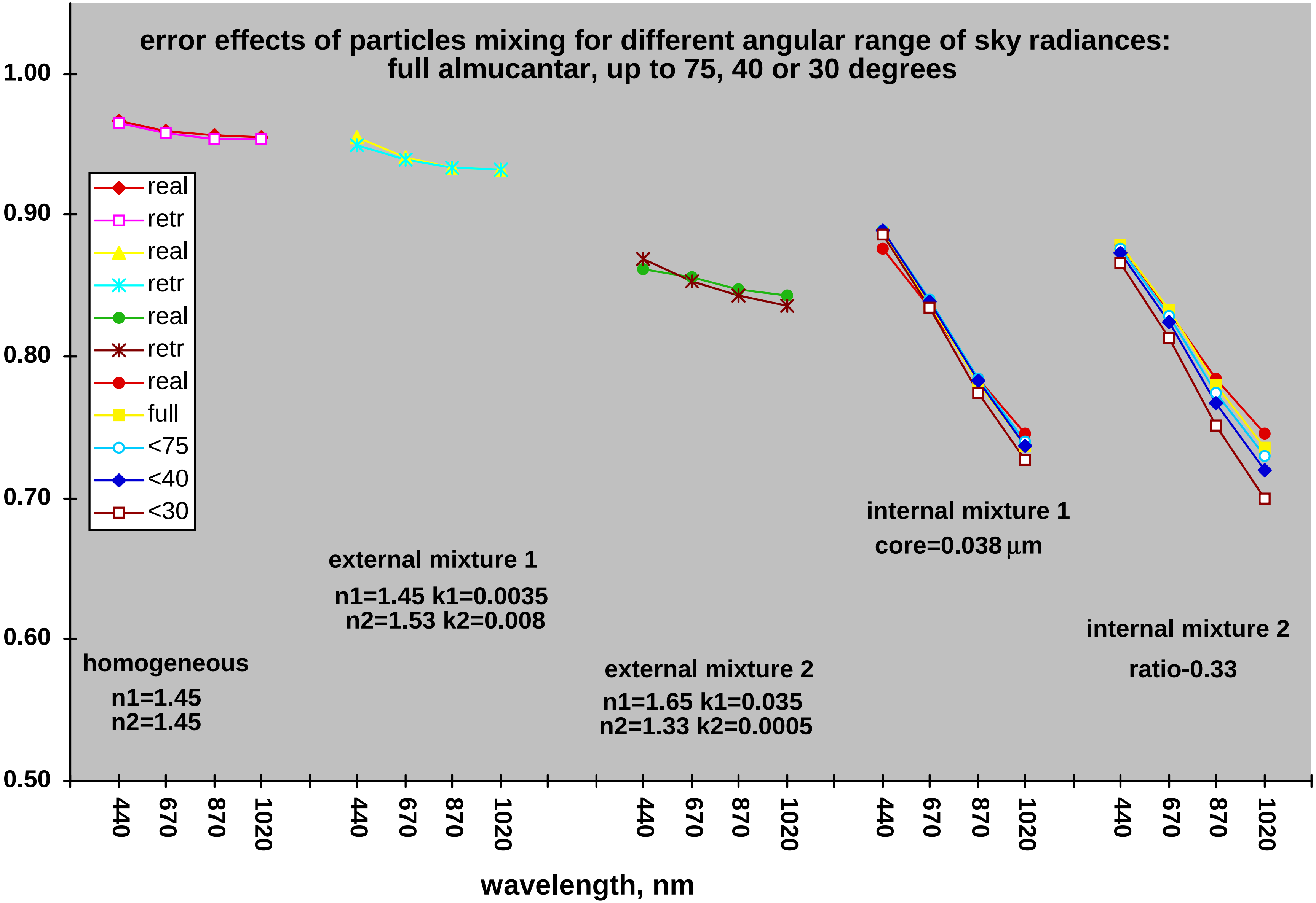
error effects of particles mixing for different angular range of sky radiances:
full almucantar, up to 75, 40 or 30 degrees
1.00
0.90
0.80
0.70
0.60
0.50
real
retr
real
retr
real
retr
real
full
<75
<40
<30
homogeneous
n1=1.45
n2=1.45
external mixture 1
n1=1.45 k1=0.0035
n2=1.53 k2=0.008
external mixture 2
n1=1.65 k1=0.035
n2=1.33 k2=0.0005
internal mixture 1
core=0.038 µm
internal mixture 2
ratio-0.33
440
670
870
1020
wavelength, nm

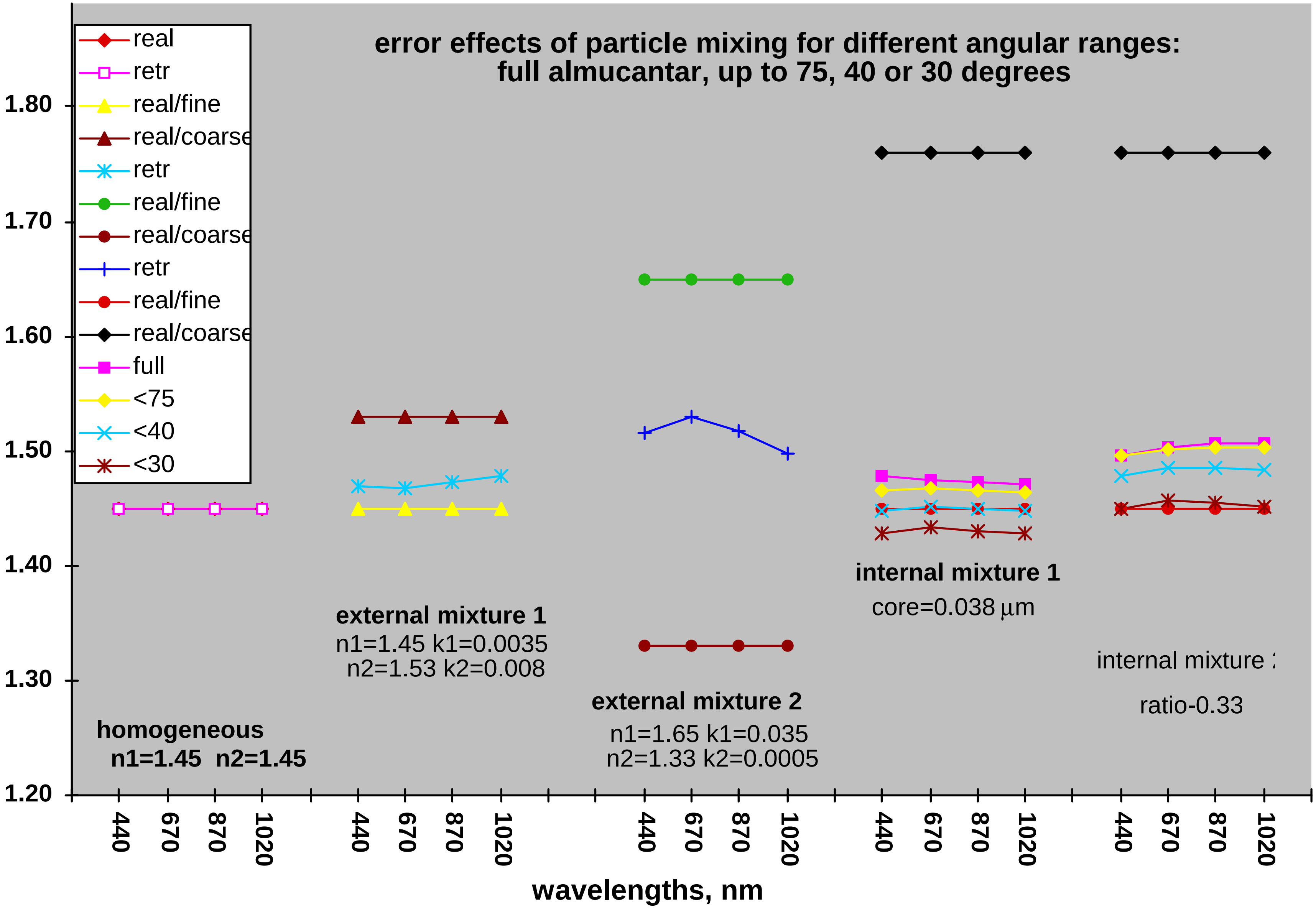
error effects of particle mixing for different angular ranges:
full almucantar, up to 75, 40 or 30 degrees
real
retr
real/fine
real/coarse
retr
real/fine
real/coarse
retr
real/fine
real/coarse
full
<75
<40
<30
1.80
1.70
1.60
1.50
1.40
1.30
1.20
homogeneous
n1=1.45 n2=1.45
external mixture 1
n1=1.45 k1=0.0035
n2=1.53 k2=0.008
external mixture 2
n1=1.65 k1=0.035
n2=1.33 k2=0.0005
internal mixture 1
core=0.038 µm
internal mixture 2
ratio-0.33
440
670
870
1020
wavelengths, nm

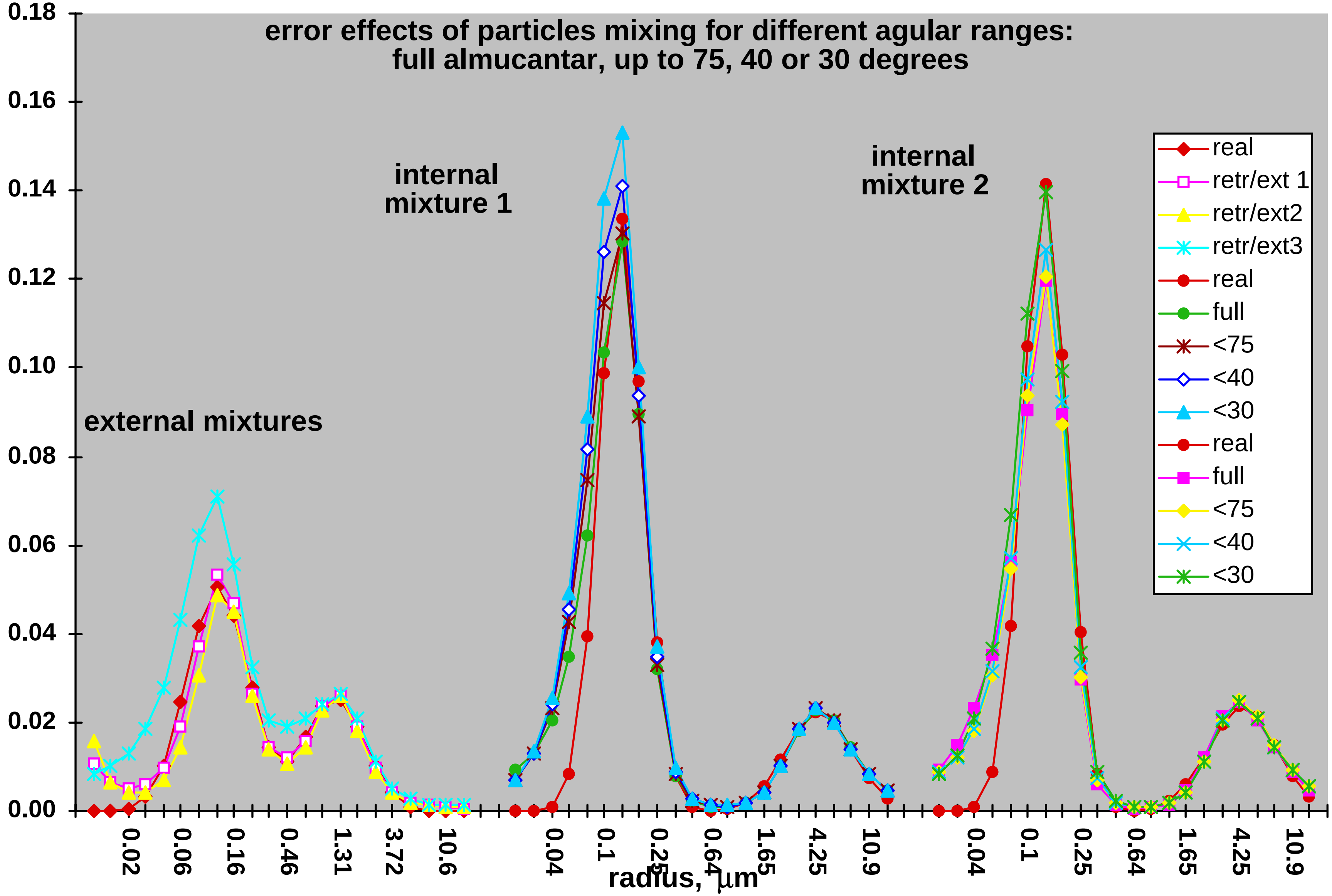

error effects of particles mixing for different agular ranges:
full almucantar, up to 75, 40 or 30 degrees
external mixtures
internal mixture 1
internal mixture 2
real
retr/ext 1
retr/ext2
retr/ext3
real
full
<75
<40
<30
real
full
<75
<40
<30
0.18
0.16
0.14
0.12
0.10
0.08
0.06
0.04
0.02
0.00
0.02
0.06
0.16
0.46
1.31
3.72
10.6
0.04
0.1
0.25
0.64
1.65
4.25
10.9
0.04
0.1
0.25
0.64
1.65
4.25
10.9
radius, μm

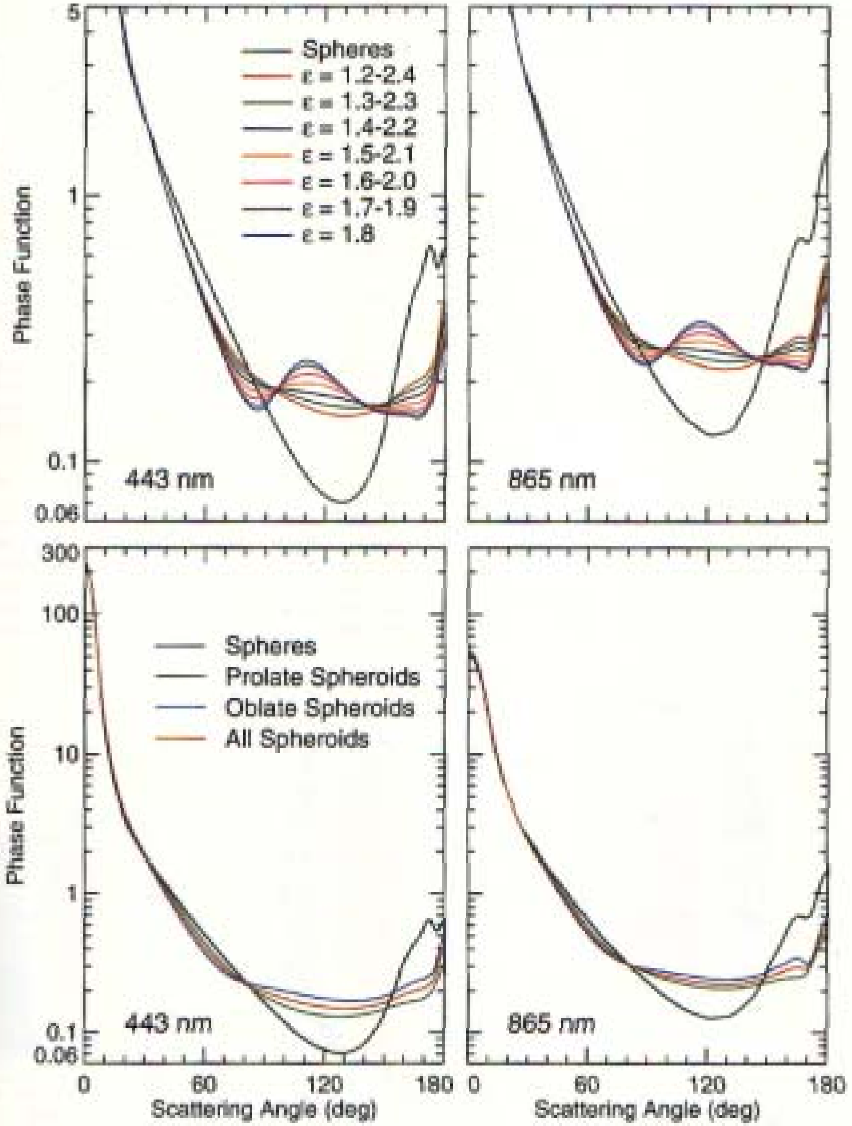

Plate 3. The upper panels demonstrate the effect of varying width of the spheroid aspect-ratio distribution and show ensemble-averaged phase functions for equiprobable shape mixtures of prolate and oblate spheroids with different aspect-ratio ranges. For all shape distributions the aspect-ratio step size is equal to 0.1. The lower panels show phase functions for polydisperse spheres and ensemble-averaged phase functions for equiprobable shape mixtures of prolate spheroids (green curve), oblate spheroids (blue curve), and prolate and oblate spheroids (red curve) with aspect ratios ranging from 1.2 to 2.4 in steps of 0.1. All curves were computed for the modified lognormal distribution of surface-equivalent-sphere radii corresponding to the accumulation mode of dustlike tropospheric aerosols (equation (9)) at wavelengths 443 and 865 nm. The spectral refractive indices are $1.53 + 0.0085i$ at 443 nm and $1.53 + 0.0012i$ at 865 nm.

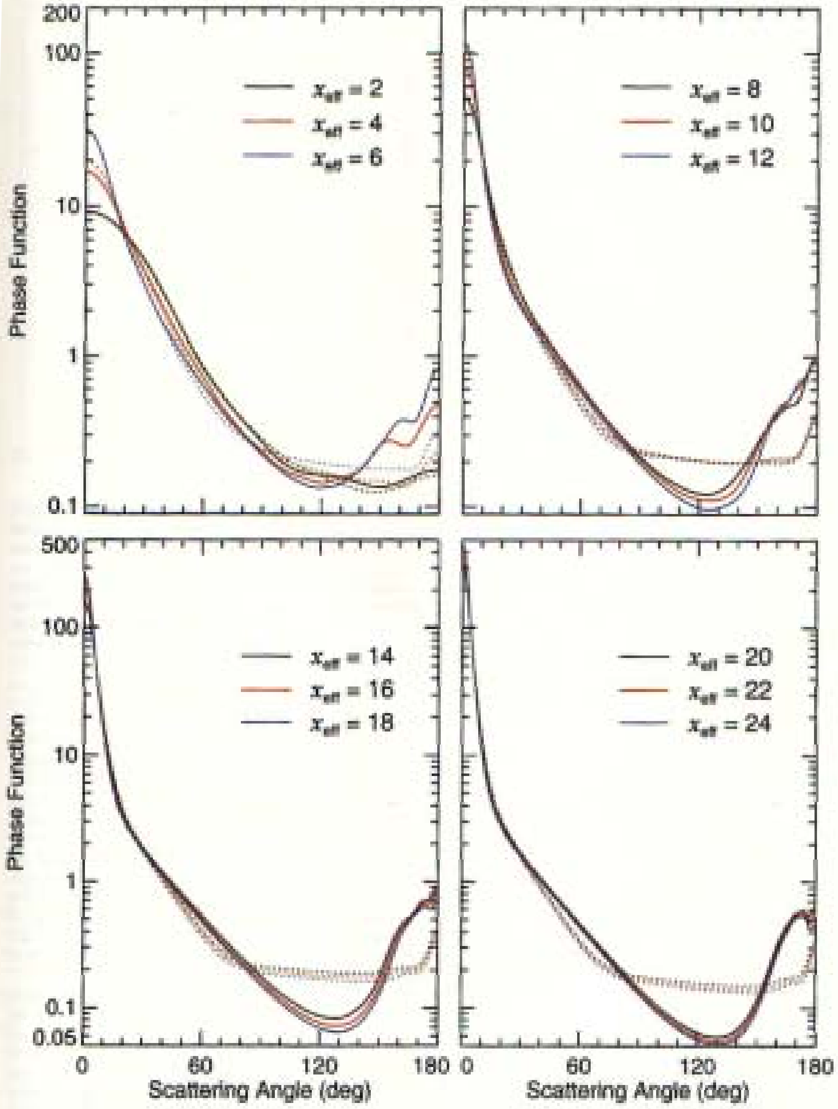

Plate 5. Phase functions for a polydisperse, equiprobable shape mixture of prolate and oblate spheroids with aspect ratios ranging from 1.4 to 2.2 in steps of 0.2 (dotted curves) and those for surface-equivalent spheres (solid curves) versus scattering angle for different values of the effective size parameter x_{eff}. The data were computed assuming the power law size distribution of equation (11) with effective variance $v_{eff} = 0.2$. The refractive index is $1.53 + 0.008i$.

Retrievals of non-spherical dust (Bahrain/ Persian Gulf)

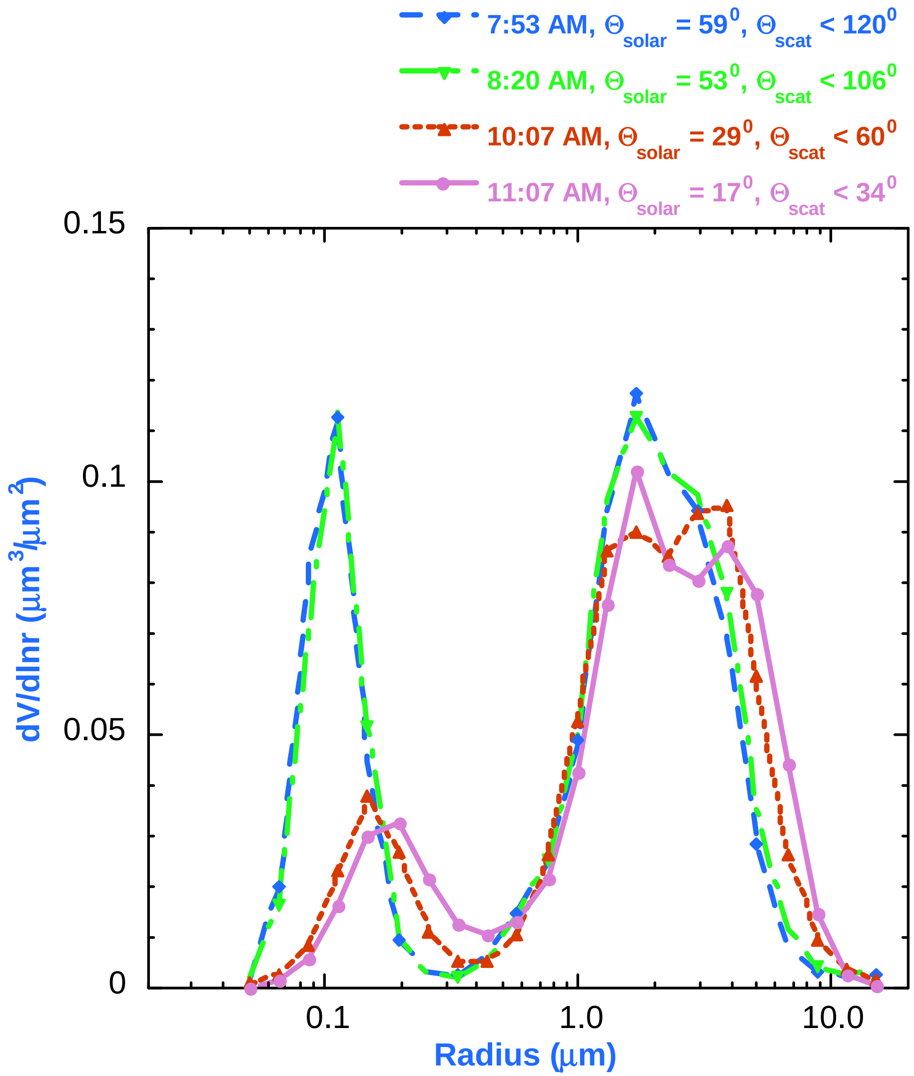

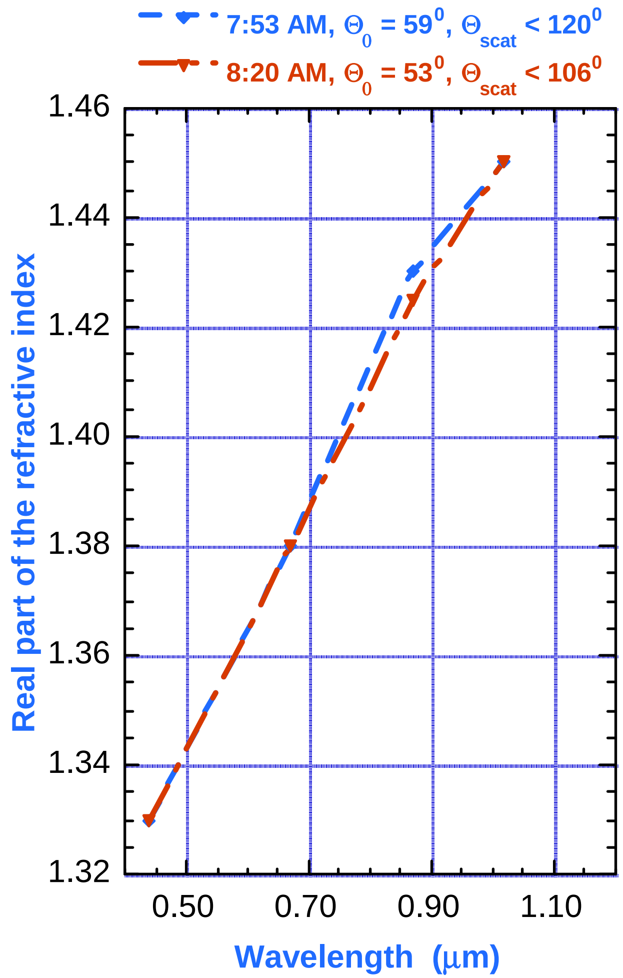

Retrieval accuracy and limitations

Sensitivity tests by Dubovik et al. 2000

Effective

bias $\Delta\tau = \pm 0.01$

	$\tau(0.44) \leq 0.2$	$\tau(0.44) \geq 0.5$
Real Part	0.05	0.025
Imaginary Part	80-100%	50%
SSA	0.05-0.07	**0.03**

Size Distribution:

Random errors

Nonsphericity biases

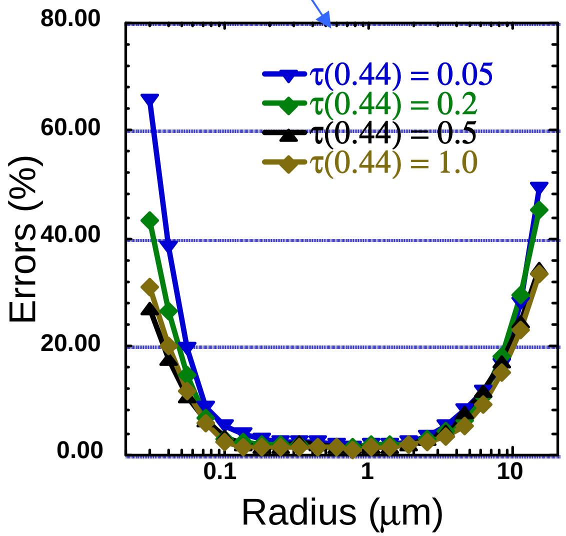

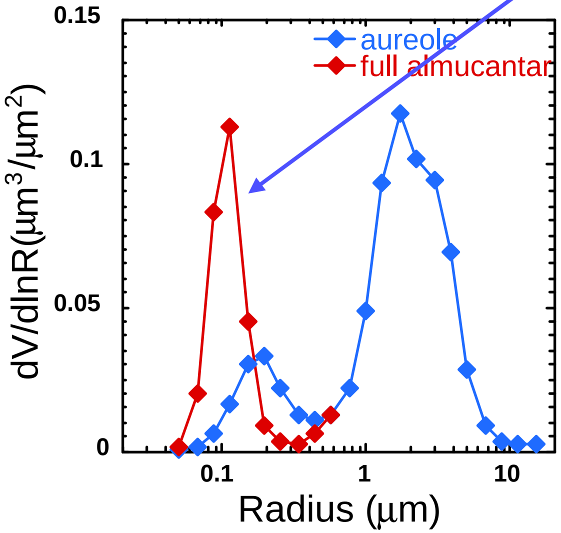

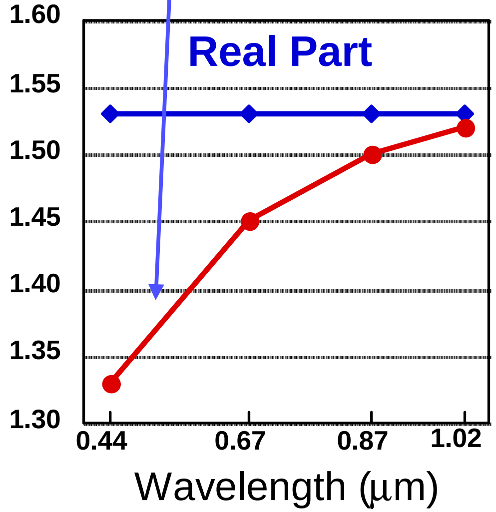

AERONET model of aerosol

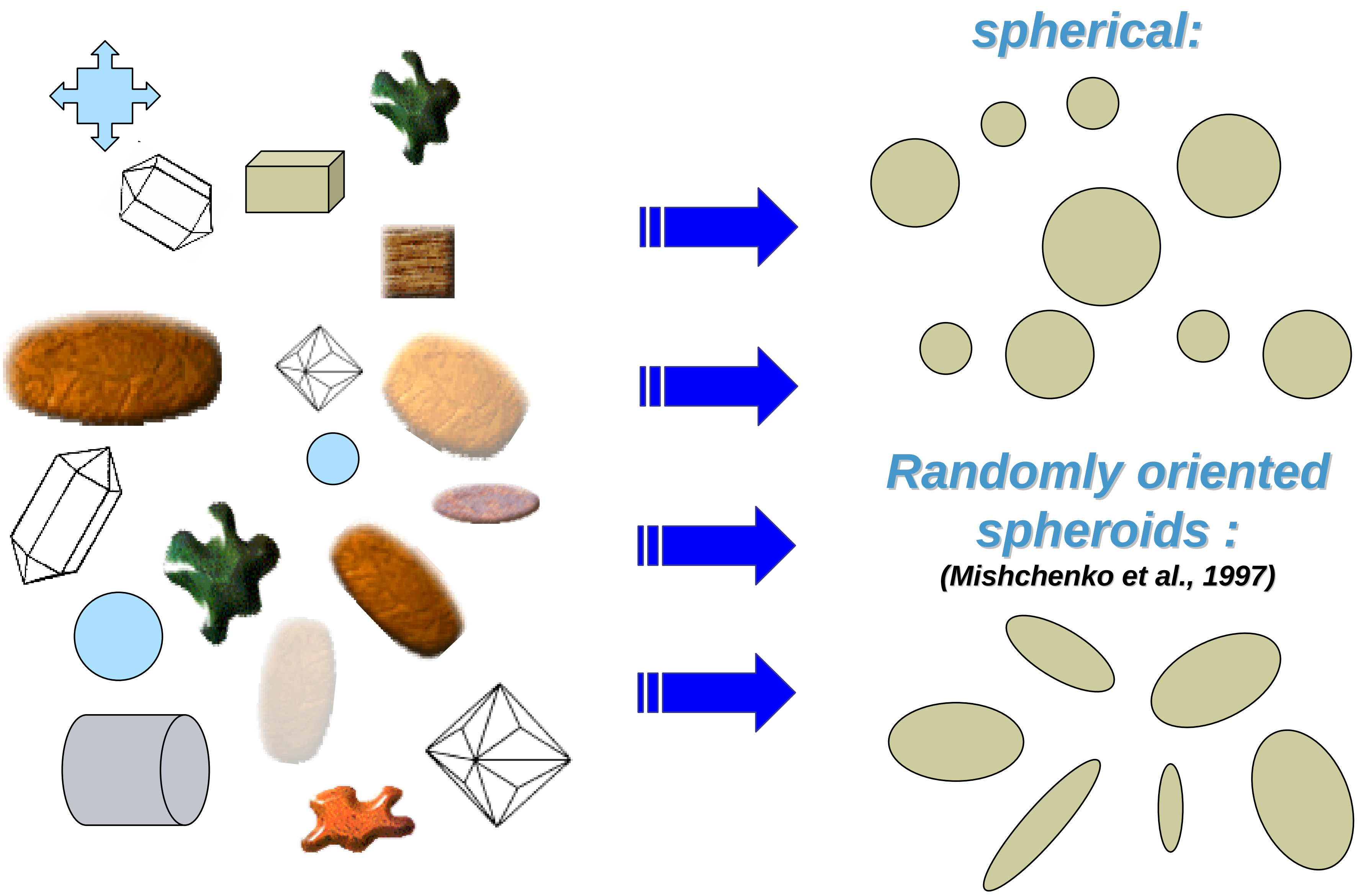

Difficulties of accounting for particle non-sphericity in aerosol retrievals:

1. The methods and programs for simulating light scattering by non-spherical particles have *many limitations* (on particle size, shape, refractive index, etc.)

2. The programs for simulating light scattering by non-spherical particles are *much slower* than Mie (spherical particle) simulations

Main limitations of T-Matrix code (Mishchenko et al.):
- size parameter ≤ ~ 60
- aspect ratio ≤ 2.4
- speed (for large aspect raitos) ~ 100 times slower than Mie

Modeling Polydispersions

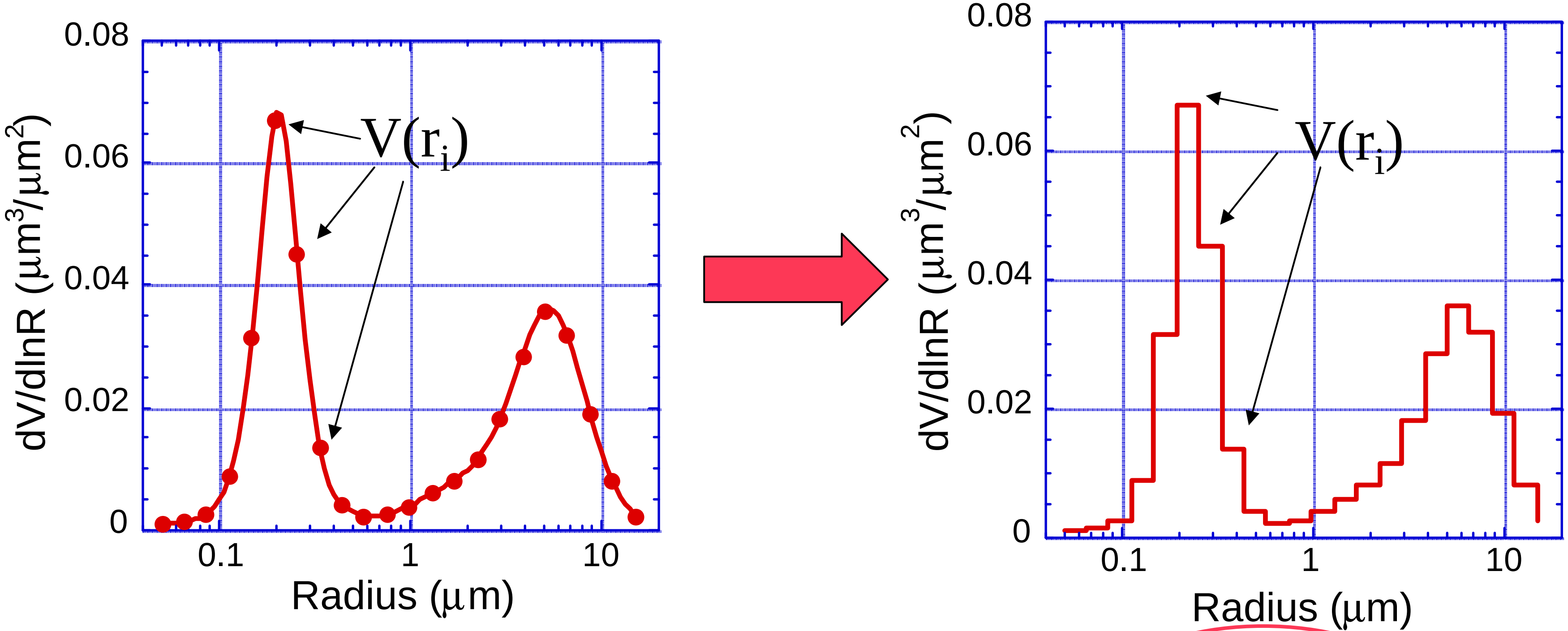

$$\tau(\lambda) = \int_{r_{\min}}^{r_{\max}} K_\tau(k;n;r)V(r)dr \approx \sum V(r_i) \int_{r_i-\Delta/2}^{r_i+\Delta/2} K_\tau(k;n;r)dr$$

$\mathbf{K}(k;n;r_i)$ - Kernel look-up table for fixed r_i (22 points)
($1.33 \le n \le 1.6$; $0.0005 \le k \le 0.5$)

Single Scattering using spheroids:

Model by Mishchenko et al. 1997:

- particles are randomly oriented homogeneous spheroids
- $\omega(\varepsilon)$ - size independent aspect ratio distribution

$$\tau(\lambda) = \int_{r_{min}}^{r_{max}} \left[\int_{\varepsilon_{min}}^{\varepsilon_{max}} K_\tau(\lambda; n; k; r; \varepsilon) V(r) \omega(\varepsilon) d\varepsilon \right] dr$$

$$\tau(\lambda) \approx \sum_{(i;p)} V_i \omega_p \left[\int_{\Delta\varepsilon_p} \int_{\Delta r_i} K_\tau(...; r; \varepsilon) dr d\varepsilon \right]$$

$$= \sum_{(i;p)} \mathbf{K}_{ip}(...; n; k) \omega_p V_i$$

K - kernel matrix:

$0.05 \leq r \leq 15$ (μm)
$1.33 \leq n \leq 1.6$
$0.0005 \leq k \leq 0.5$
$1.2 \leq \varepsilon \leq 2.2$

Computational challenge of using spheroids

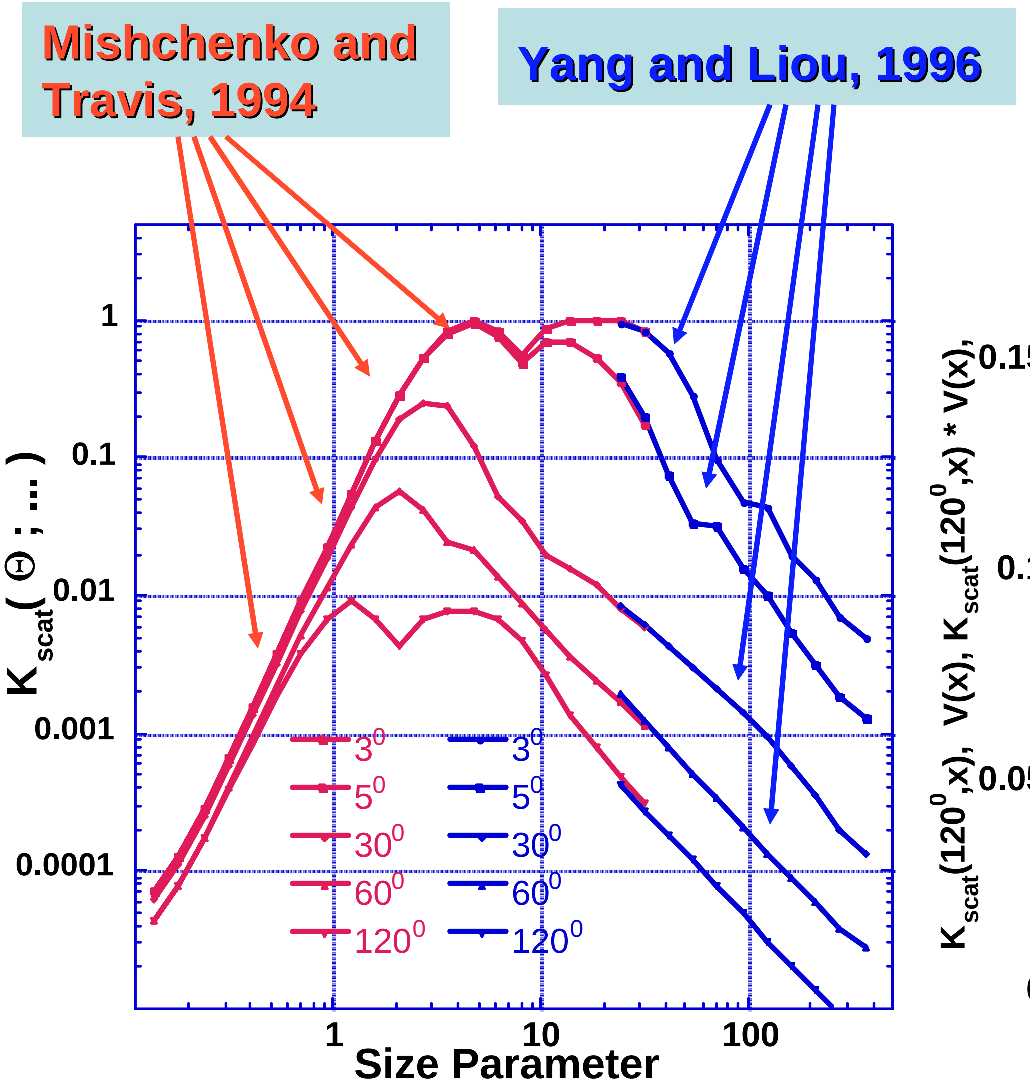

Contribution of different sizes to scattering at 120^0

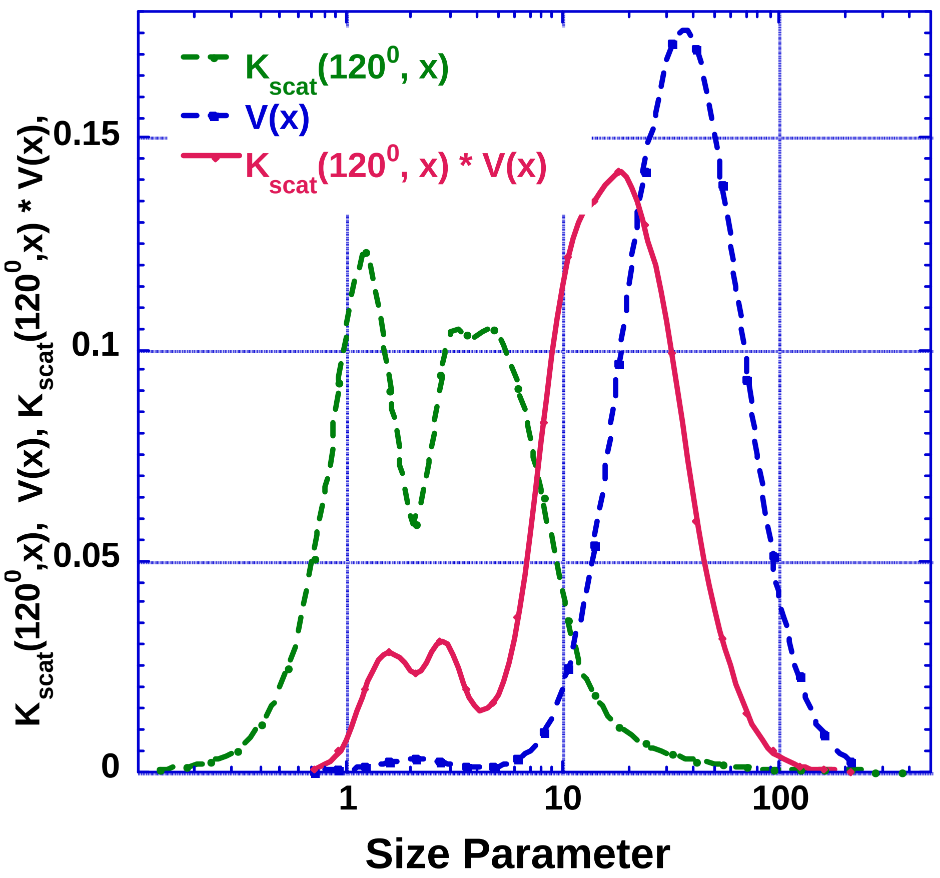

Yang et al. 2000

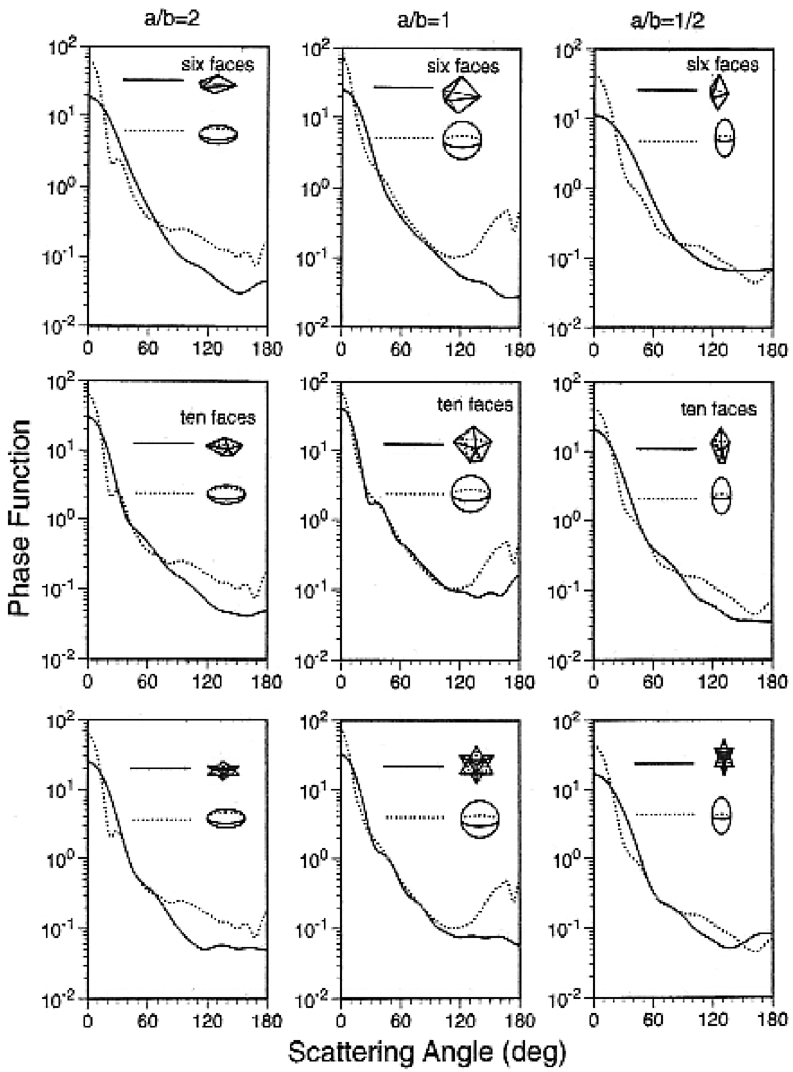

Fig. 9. Comparison of the phase functions for oceanic aerosol particles of various shapes. For spherical particles, i.e., $a/b = 1$, a power-law size distribution is employed to smooth out the resonant fluctuations. The size parameter used is $x_{\max} = 10$.

Improved dust retrievals using spheroids:

Contributors:
Lapyonok, Mishchenko, Yang, Sinyuk

Real Refractive Index

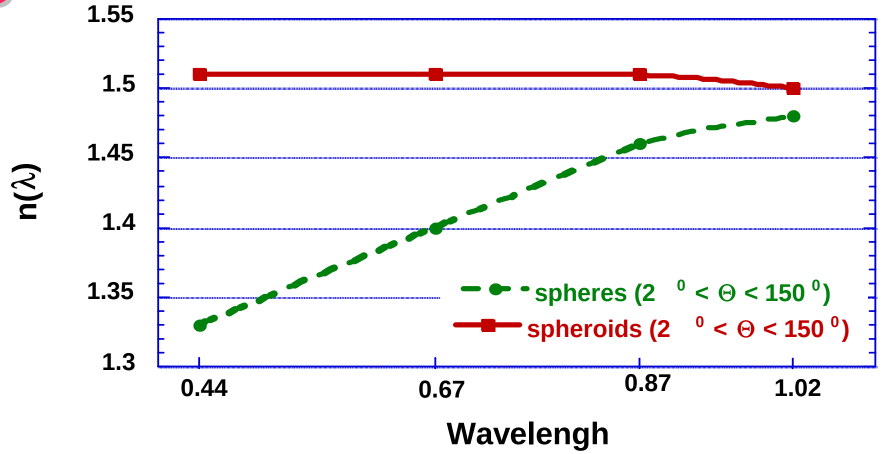

Size Distribution

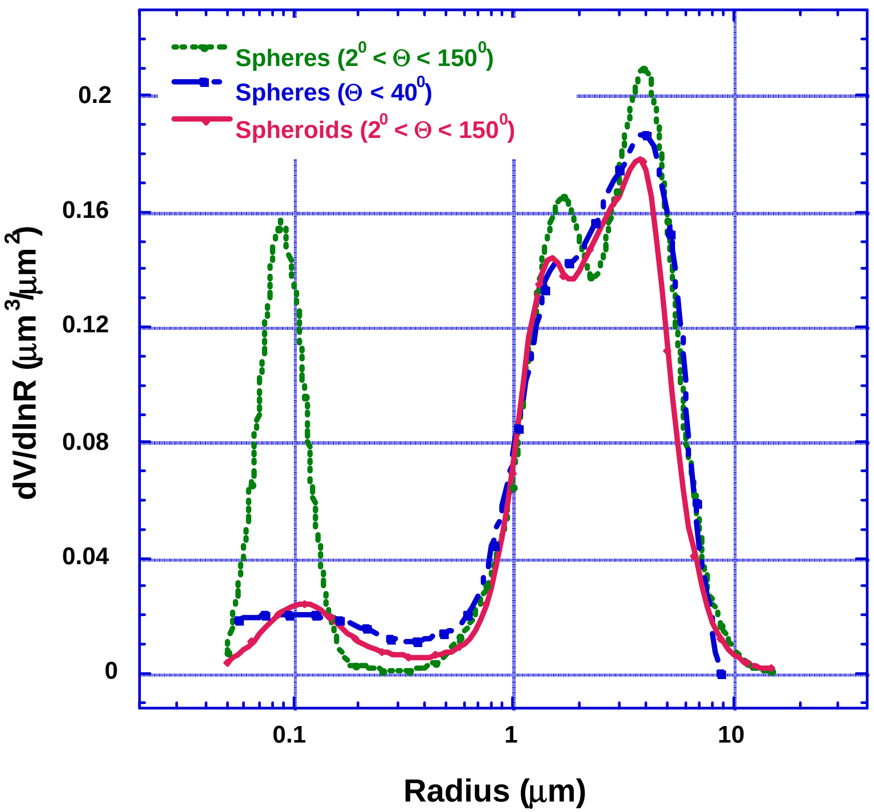

Phase Function

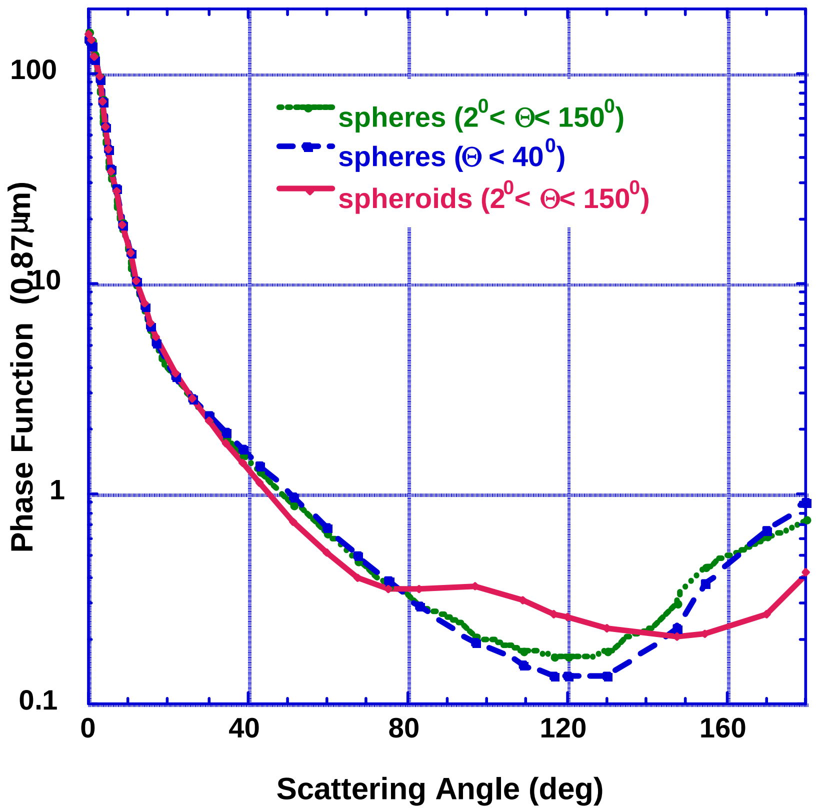

Cape Verde (2001) dust
Size distributions

(110 cases; $\tau(1020) \geq 0.3$; $\alpha \leq 0.6$)

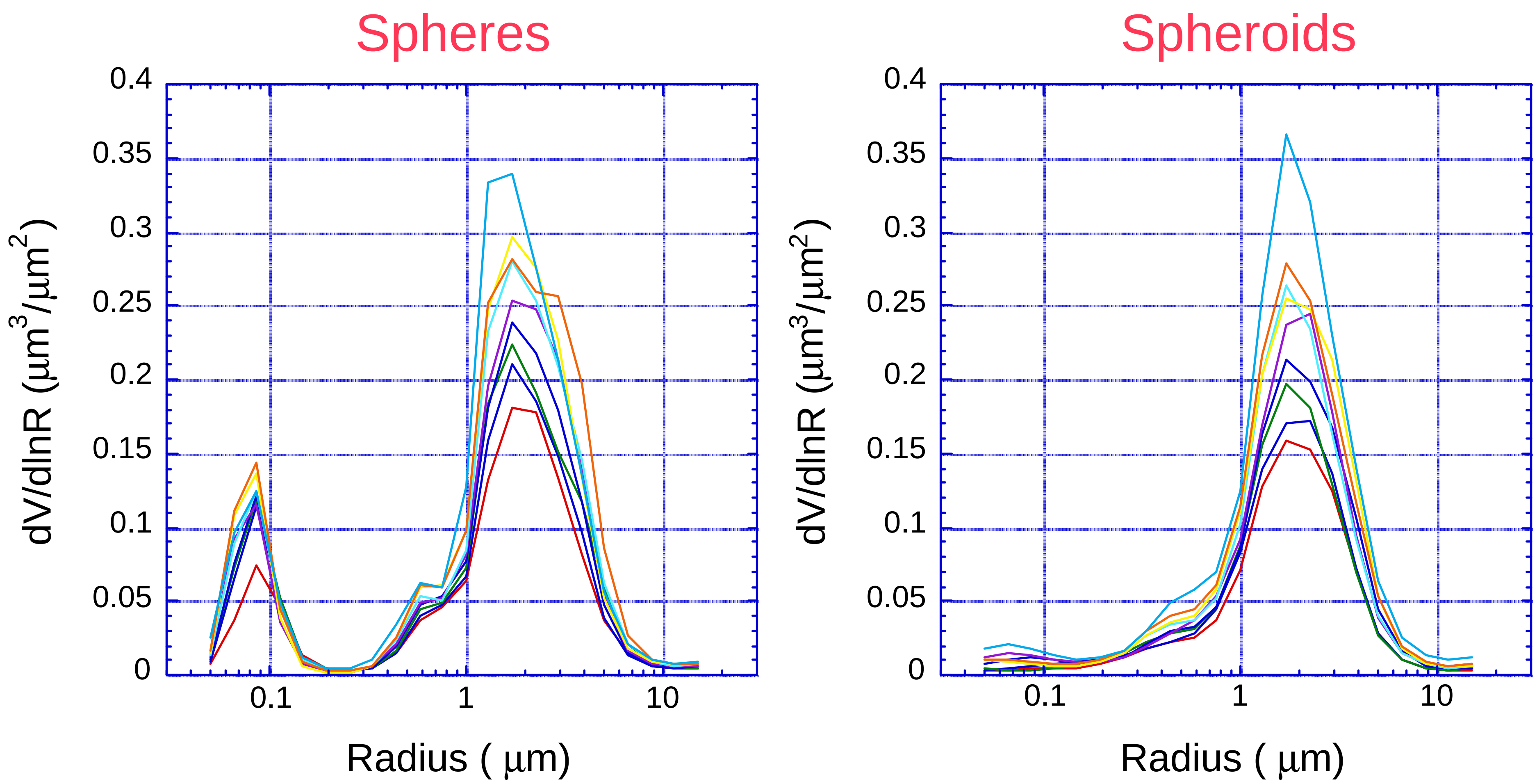

9 groups: τ = 0.39, 0.44, 0.48, 0.50, 0.52, 0.57, 0.60, 0.62,0.71

Cape Verde (2001) dust

ω_0 and $n(\lambda)$ (averaged)

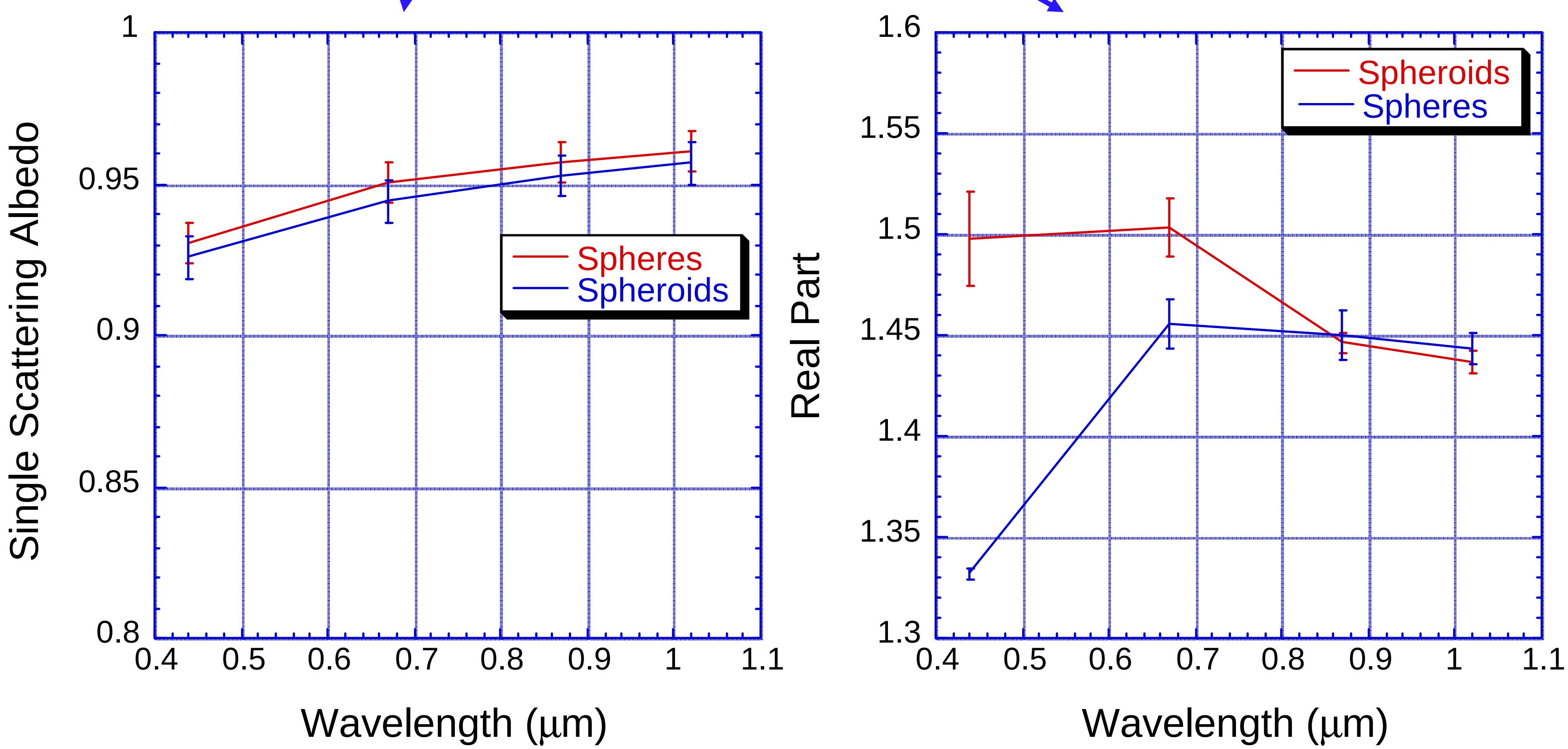

No shape effect on Fine mode aerosols :

Spheres versus Spheroids

Real Part of the Ref. Index

Single Scattering Albedo

Size Distribution

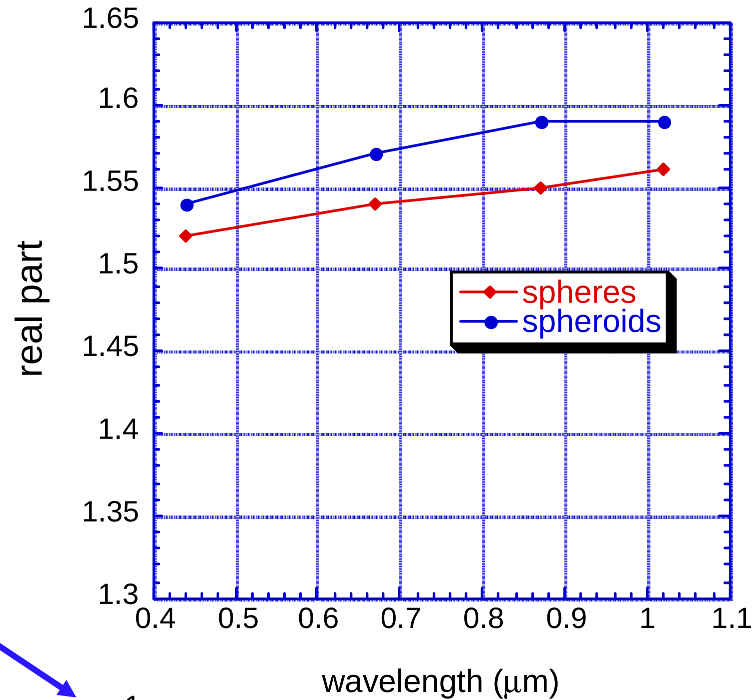

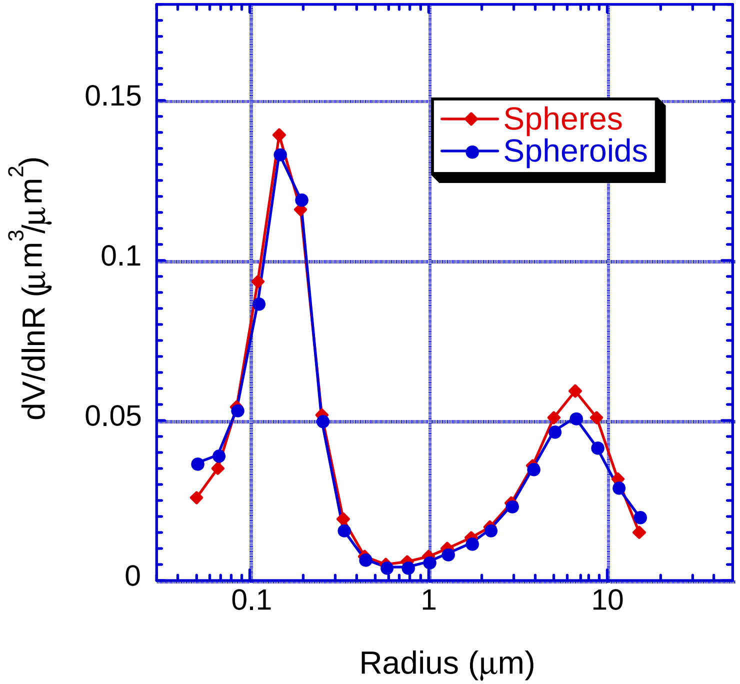

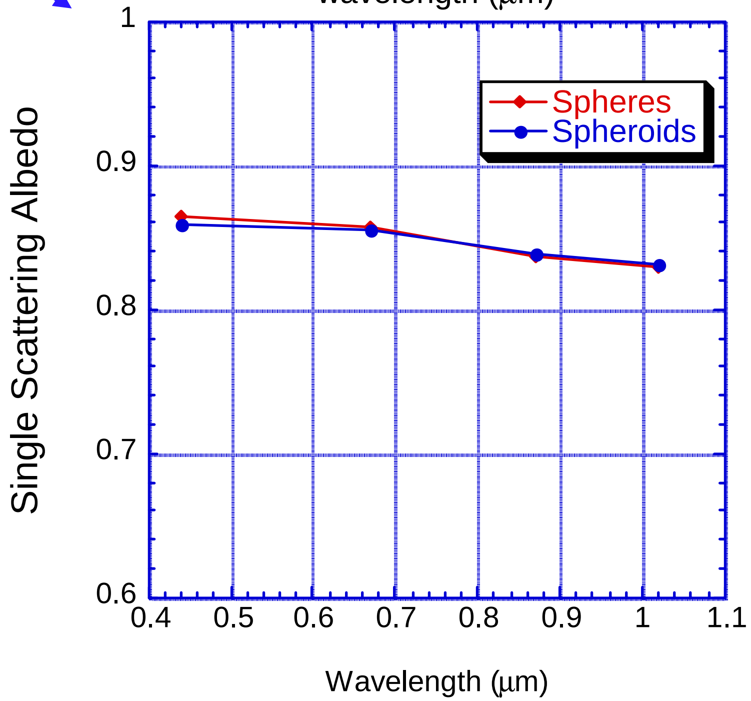

Differences in Phase Functions due to particle non-sphericity

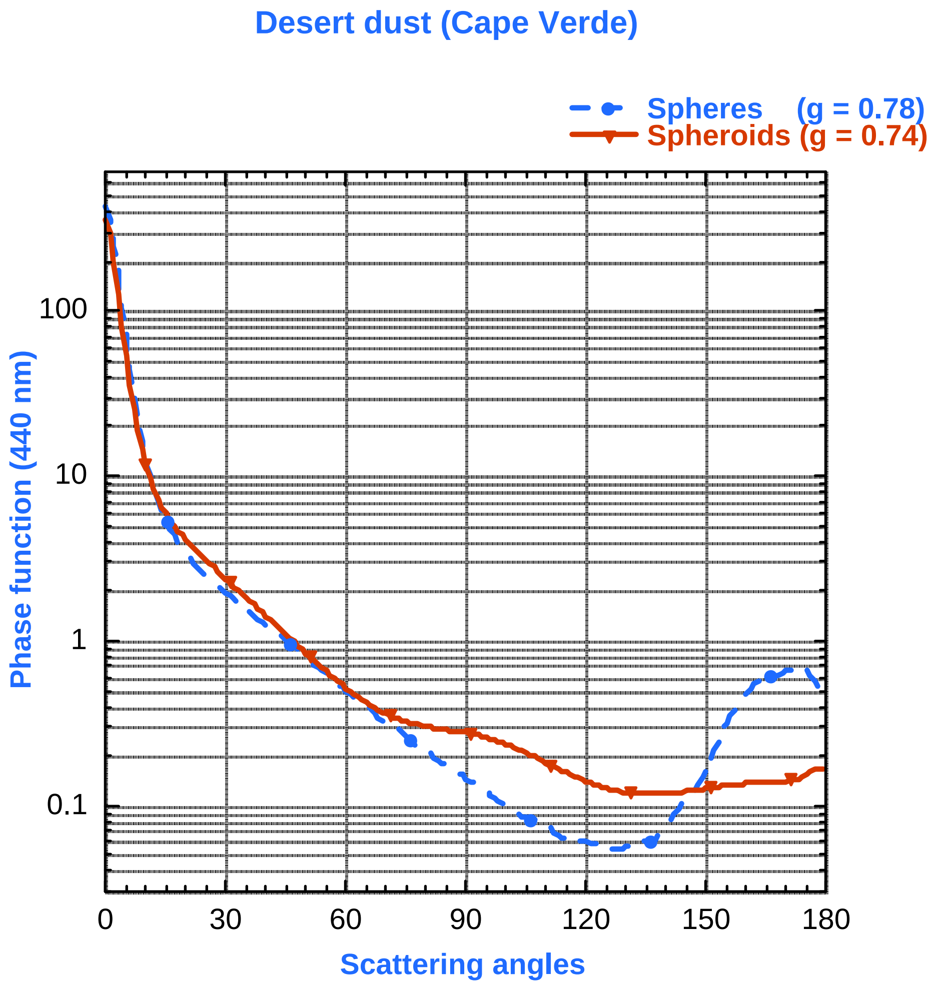

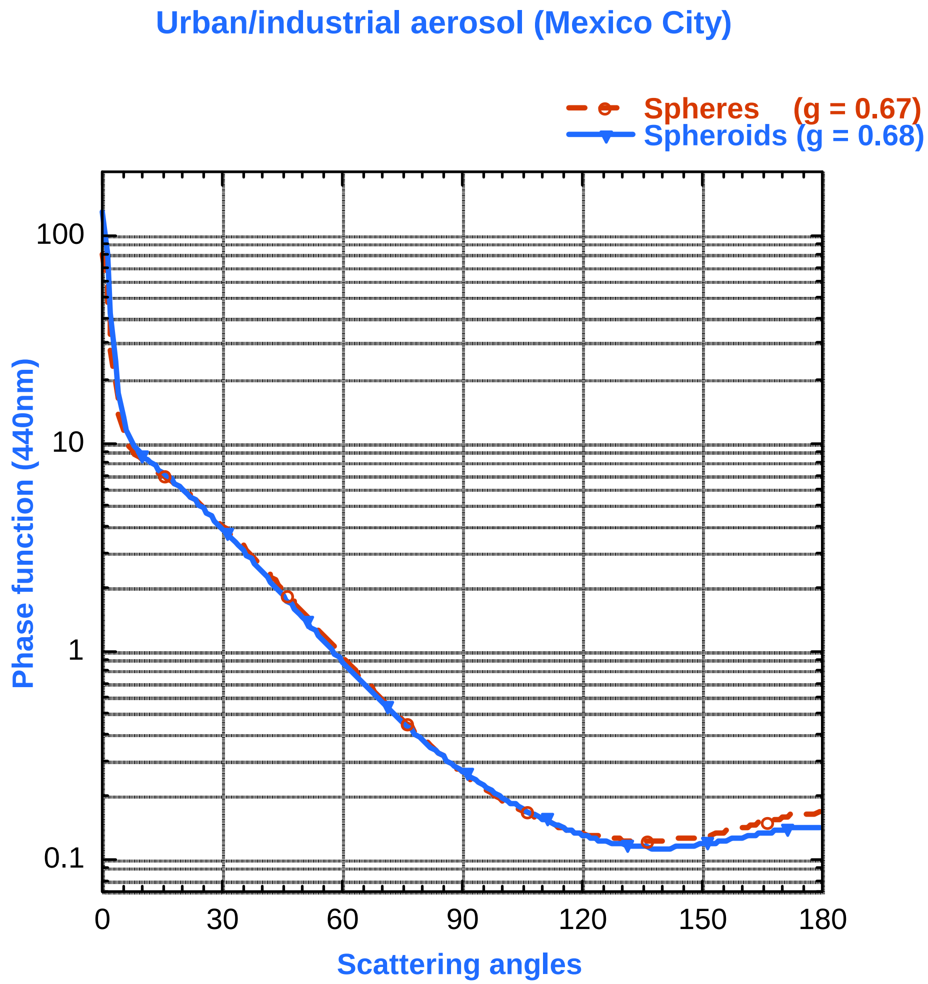

Aspect Ratio Distribution

Distribution Shape -?,
Distribution Size Dependence - ?

Mishchenko et al. 1997
and this work

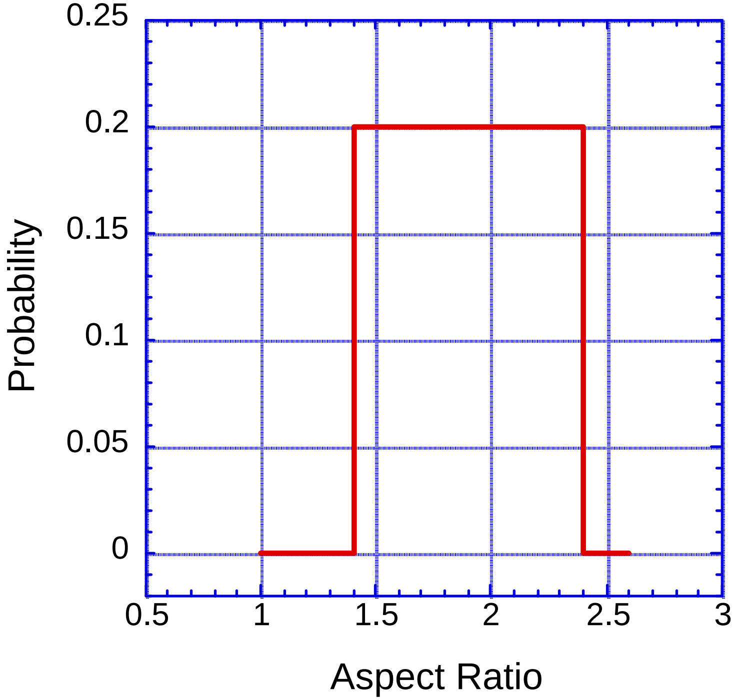

C. Cattrall, 2002

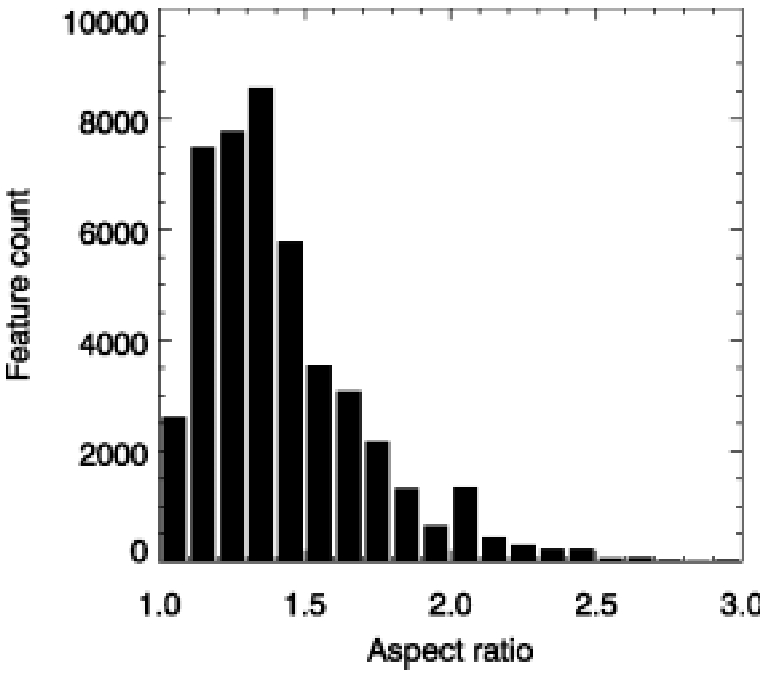

Conclusion:

Capable retrievals ($dV/d\ln r$, $n(\lambda)$,$k(\lambda)$, $\omega_0(\lambda)$, $P(\lambda;\Theta)$, etc.)**:**

- *optimized inversion*
- *elaborated forward model (with* ***non-spherical particle shape****);*
- *extensive sensitivity tests*

Aerosol climatology under establishment:

- *dynamic aerosol models* ($dV/d\ln r$, $n(\lambda)$, $k(\lambda)$, $\omega_0(\lambda)$, $P(\lambda;\Theta)$, etc.)**:**

Future plans and additional development:

- *extended spectral range; polarization; improving non-spericity;*
- *including particle shape into dynamic models;*

Data integrations *(in proposals)* **:**

- ***multi-instrument*** *aerosol retrieval:*

  AERONET + CAR + MODIS+ MISR…

- *assimilating* ***MODIS+AERONET with GOCART*** *transport model*

Comparison of Phase Matrices: spheres and randomly oriented spheroids (prolate/oblate, 1.4 <ε< 2.2) for Saudi Arabia dust model [Dubovik et al. 2002] versus average measurements [Volten et al. 2001]

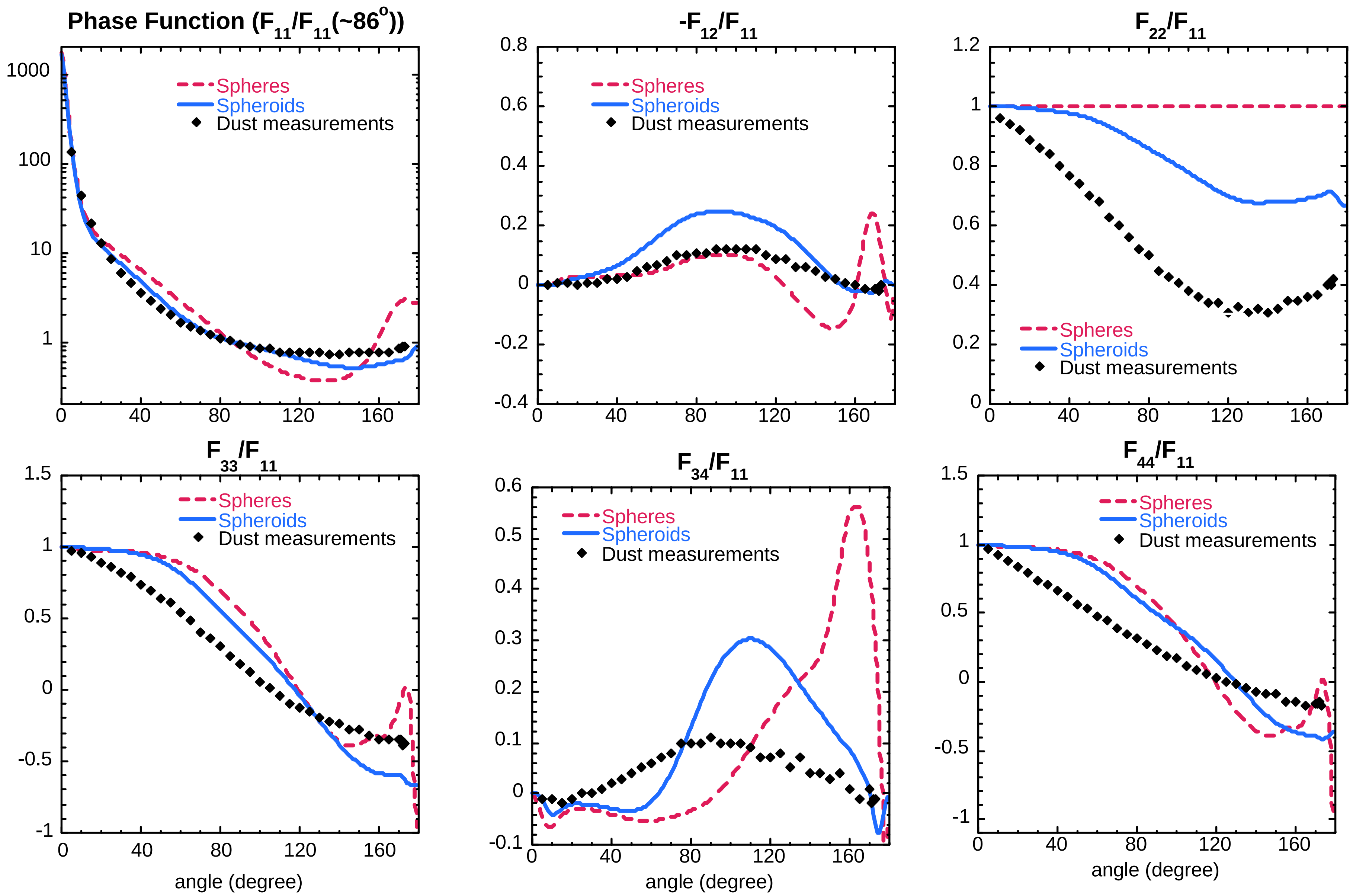

__Contributors:__

Kaufman, Ginoux, Lapyonok, Chin

Global Measurements:

Assimilation of aerosol measurements

Input to GOCART: emission sources

AEROSOL properties by GOCART

MODIS optical thickness at 1.24 μm

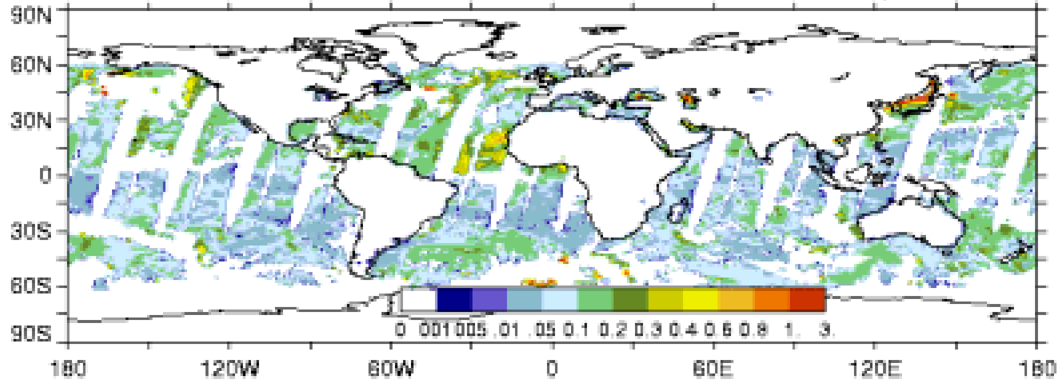

Mass emission (kg/cell: $10^0 X 10^0$/20 min)

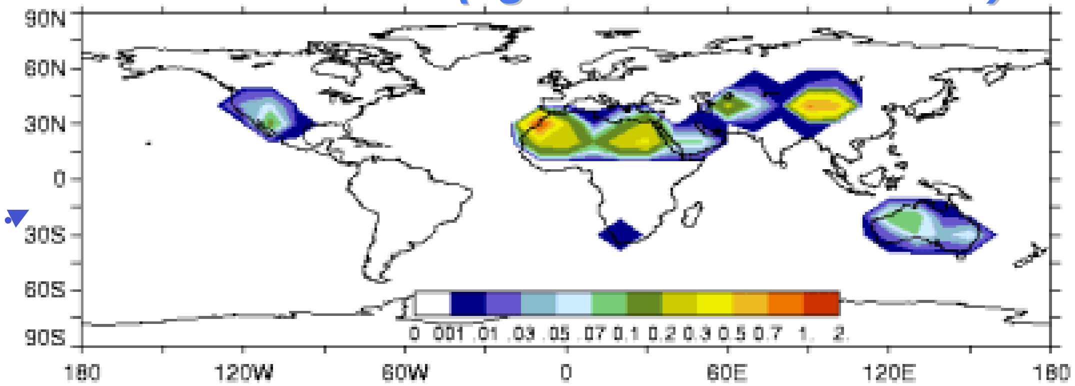

GOCART optical thickness at 1.24 μm